SPE
Society of Petroleum Engineers

SPE 14237

Case Study of a Low-Permeability Volatile Oil Field Using Individual-Well Advanced Decline Curve Analysis

by M.J. Fetkovich, *Phillips Petroleum Co.*; M.E. Vienot, *Phillips Petroleum Co. Europe-Africa*; and R.D. Johnson and B.A. Bowman, *Phillips Oil Co.*

SPE Members

This paper was prepared for presentation at the 60th Annual Technical Conference and Exhibition of the Society of Petroleum Engineers held in Las Vegas, NV September 22-25, 1985.

ABSTRACT

This paper presents a detailed case history study of a low permeability volatile oil field located in Campbell County, Wyoming. The field was analyzed on an individual well basis using advanced decline curve analysis for 40 individual well completions. Well permeabilities, skins and original oil in place are calculated for each well from rate-time analysis using constant wellbore pressure type curve analysis techniques.

Original oil in place values calculated from rate-time analysis for individual wells are used with recoverable reserve projections from the decline analysis to obtain fractional recoveries for each well. Gas-oil ratios versus fractional recovery curves are also made for each well using historical cumulative production and the calculated oil in place values. Ultimate fractional recovery numbers and GOR vs fractional recovery curves, plotted for each well, are shown to suggest different rock types and reservoir fluids. Multi-well decline curve analysis shows the validity of the variables s (skin), k, OOIP, ultimate fractional recovery and GOR vs fractional recovery evaluated from each well's type curve evaluation. These variables must all give consistent and reasonable numbers when compared with each other. A single well analysis can easily give results that are not recognized as being invalid unless compared with other wells in the field.

The study also illustrates flowing and pumping well backpressure changes in a well's decline, the method of handling such changes, and their effect on ultimate recoverable reserves predictions. Conventional decline curve analysis can not handle backpressure changes because of its constraint that what controls the decline in the past will also continue in the future.

References and illustrations at end of paper.

INTRODUCTION

In solution gas drive reservoirs, decline curve analysis of rate-time data for predicting future production and determining recoverable reserves for a fairly large number of wells is commonly done using the Arps[1] empirical equations and a computerized statistical approach to arrive at answers fairly quickly. For wells in high permeability reservoirs producing essentially wide-open, without future backpressure changes and without future stimulation treatments, the results obtained should be reasonably good providing the limits of the decline exponent b of between 0 and 1.0 are honored.

At the other extreme in analyzing rate-time data for predicting future production and recoverable reserves, a reservoir simulation study could be undertaken. However, this approach could take as much as a year to accomplish and normally would not be considered acceptable, particularly for time-constrained property acquisition or sales situations where few of the detailed reservoir parameters necessary for a simulation study are available.

Many of the newer oil and gas fields being discovered and produced are in the low permeability classification, where transient behavior can last for years, and therefore are not amenable to analysis using the Arps equation alone. Also, a model study of such low permeability reservoirs would require a very fine grid system to correctly simulate and match the early transient rate-time decline data.

An approach to the problem of analyzing low permeability wells and total field rate-time decline has been given in papers[2 3 4 5 6] that illustrate methods of handling both the transient and depletion stages of rate-time decline. Well permeabilities, skins from stimulation treatments and original oil in place or original gas-in-place can be calculated for each well from rate-time data using constant wellbore pressure type curve analysis techniques.

With a field case study of the School Creek Field in Campbell County, Wyoming, a low permeability volatile oil field, we will present a stepwise procedure for doing a total field study using individual well advanced decline curve analysis techniques. Original oil in place values calculated from rate-time analysis for individual wells are used with recoverable reserve projections from the decline analysis to obtain fractional recoveries for each well. Gas-oil ratio versus fractional recovery curves are also made for each well using historical cumulative production and the calculated oil in place values. Ultimate fractional recovery values and GOR versus fractional recovery curves, plotted for each well, are shown to suggest different rock types and reservoir fluids. Multi-well decline curve analysis shows the validity of the variables s (skin), k, OOIP, ultimate fractional recovery and GOR versus fractional recovery evaluated from each well's type curve match point. These variables must all give consistent and reasonable numbers when compared with each other. A single well analysis can often give results that are not recognized as being invalid unless compared with several other wells in the field. The study also includes and illustrates flowing and pumping well backpressure changes in a well's decline, the method of handling such changes and their effect on ultimate recoverable reserves predictions. Conventional decline curve analysis approaches do not consider backpressure changes and their effect on projected recoverable reserves.

School Creek Field - Wyoming

The School Creek Field is located on the eastern flank of the south central portion of the Powder River Basin in Campbell and Converse Counties, Wyoming. Following deposition of the underlying Skull Creek Shale, the lower Cretaceous sea receded from the area of the Powder River Basin. Subsequently, a wide-spread drainage system developed and carved its pattern into the Skull Creek Shale. As the lower Cretaceous sea transgressed east, Muddy deltaic sediments buried the previously deposited channel sediments as the sea continued to inundate the basin. Continuous basin fill by deposition of the overlying Mowry Shale resulted in the Muddy reservoir sands being ideally "sandwiched" between two marine hydrocarbon source shales.

In the School Creek Area, a north-south paleodrainage pattern was developed upon the underlying Skull Creek Shale and controlled the distribution of the productive tidal channel and point-bar sands of the lower Muddy formation. Younger upper Muddy marine facies units were then deposited as the Cretaceous sea transgressed east resulting in some well developed productive marine offshore bar sands within the field area.

In the School Creek Field, the Lower Muddy channel sands have 35 well completions with an average of 11 net feet of pay per well and an average porosity and water saturation of 13.6% and 39%, respectively. Upper Muddy bar sands have 5 well completions with an average of 12 net feet of pay per well and an average porosity and water saturation of 22% and 14%, respectively. Production has also been established in secondary objectives, which include the Sussex, Turner, and Dakota formations. These wells are not included in this study.

Figure 1 is a plat showing the well locations, their relationship to the Channel Sand and Bar Sand and the three wells from which PVT samples were taken. Figure 2 is a type log for a School Creek Field Muddy formation completion.

The School Creek Field was discovered in 1980 when the Matheson E-1 well was drilled to 10,000 feet and completed in the Muddy formation. The initial reservoir pressure was approximately 3700 - 3600 psi. Basic fluid properties are given from three different PVT studies in Table 2 and Figure 3. Two quite different fluid samples were obtained in the Channel Sand: the Federal EE-1 sample with a bubble point pressure of 3400 psi, GOR of 1557 SCF/BBL and the Matheson E-1 sample with a bubble point pressure of 2705 psi, GOR of 736 SCF/BBL. Based on reported initial producing gas-oil ratios, the Federal EE-1 sample was used to represent wells in the southern portion of the field while the Matheson E-1 sample was used for wells in the northern portion of the field. The Federal J-1 sample was only used to represent the five Bar Sand well completions. Its bubble point pressure was 2838 psi with a gas-oil ratio of 1189 SCF/BBL.

Basic Decline Analysis Equations

The Arps[1] empirical decline equations that can be used for analysis and forecasting future production when depletion is clearly indicated are, for

$b > 0$

$$q(t) = \frac{q_i}{[1 + bD_i t]^{1/b}} \qquad \text{................(1)}$$

and for $b = 0$ (exponential)

$$q(t) = \frac{q_i}{e^{D_i t}} \qquad \text{................(2)}$$

where the limits of b are between 0 and 1.

For type curve analysis

$$q_{Dd} = \frac{q(t)}{q_i} \qquad \text{................(3)}$$

and

$$t_{Dd} = D_i t \qquad \text{................(4)}$$

From log-log type curve matching, the match of the rate-time data yields b, $t - t_{Dd}$, and $q(t) - q_{Dd}$. From these values q_i and D_i are evaluated and can then be used in the predictive equations 1 or 2 above to forecast future production and to obtain ultimate recoverable reserves.

As given in reference 3, we can also evaluate the productivity factor from $q(t) - q_{Dd}$ match point, the <u>same</u> match point as would be used with the above Arps equations.

$$P.F. = \frac{kh}{\left[\ln\left(\frac{r_e}{r_w'}\right) - \frac{1}{2}\right]} = \frac{141.2\ (\overline{\mu\beta})}{\overline{p}_R - p_{wf}} \cdot \frac{q(t)}{q_{Dd}} \quad ...(5)$$

where r_w' is the effective wellbore radius incorporating the skin term, $r_w' = r_w\, e^{-s}$. The skin term can also include the effect of a shape factor C_A. See reference 7. If r_e/r_w' can be defined from a match of early transient data, we could then evaluate k and s of the well.

To evaluate pore volume[3], V_p, from the match point, we have

$$V_p = \pi\, r_e^2 h\phi = \frac{(\overline{\mu\beta})}{(\mu c_t)_{\overline{p}_R}(\overline{p}_R - p_{wf})} \cdot \frac{t}{t_{Dd}} \cdot \frac{q(t)}{q_{Dd}} \quad ...(6)$$

which gives the pore volume at the <u>start</u> of the decline analysis.

In the above equations, $(\overline{\mu\beta})$ is normally evaluated at average pressure $(\overline{p}_R + p_{wf})/2$ while (μc_t) is evaluated at reservoir shut-in pressure $\overline{p}_R$.

In terms of an oil pseudo pressure, $m(p)_{oil}$, equations 5 and 6 can be written as

$$\frac{kh}{\left[\ln\left(\frac{r_e}{r_w'}\right) - \frac{1}{2}\right]} = \frac{141.2}{m(\overline{p}_R) - m(p_{wf})} \cdot \frac{q(t)}{q_{Dd}} \quad ....(7)$$

and $$V_p = \frac{1}{(\mu c_t)_{\overline{p}_R}\ [(m(\overline{p}_R) - m(p_{wf})]} \cdot \frac{t}{t_{Dd}} \cdot \frac{q(t)}{q_{Dd}} \quad ...(8)$$

Using a simple, practical engineering $m(p)_{oil}$ defined from inflow performance relationships, sufficient for decline curve analysis, (see Appendix), we would have for $\overline{p}_R \leq p_b$ (bubble point pressure)

$$\frac{kh}{\left[\ln\left(\frac{r_e}{r_w'}\right) - \frac{1}{2}\right]} = \frac{141.2\ (2\overline{p}_R)(\mu\beta)_{\overline{p}_R}}{(\overline{p}_R^{\ 2} - p_{wf}^2)} \cdot \frac{q(t)}{q_{Dd}} \quad ...(9)$$

and $$V_p = \frac{2\overline{p}_R\ (\beta)_{\overline{p}_R}}{(c_t)_{\overline{p}_R}\ (\overline{p}_R^{\ 2} - p_{wf}^2)} \cdot \frac{t}{t_{Dd}} \cdot \frac{q(t)}{q_{Dd}} \quad ...(10)$$

Note that $\mu\beta$ is now evaluated at reservoir shut-in pressure, $\overline{p}_R$, as is (μc_t), which then allows cancellation of the viscosity terms in equation 10.

For cases where $p_{wf} < p_b$ and $\overline{p}_R > p_b$, as is the case for most of the School Creek Field wells in this study, the productivity factor is evaluated from

$$\frac{kh}{\left[\ln\left(\frac{r_e}{r_w'}\right) - \frac{1}{2}\right]} = \frac{141.2\ (\mu\beta)_{\overline{p}_R}}{\left[(\overline{p}_R - p_b) + \frac{(p_b^2 - p_{wf}^2)}{2p_b}\right]} \cdot \frac{q(t)}{q_{Dd}} \quad (11)$$

and

$$V_p = \frac{(\beta)_{\overline{p}_R}}{(c_t)_{\overline{p}_R}\left[(\overline{p}_R - p_b) + \frac{(p_b^2 - p_{wf}^2)}{2p_b}\right]} \cdot \frac{t}{t_{Dd}} \cdot \frac{q(t)}{q_{Dd}} \quad (12)$$

Equations 11 and 12 reduce to a simple Δp^2 form when $\overline{p}_R \leq p_b$ (see for example equation A-9 in the Appendix).

To calculate a drainage radius from the pore volume, we have

$$r_e = \sqrt{\frac{V_p \times 5.615}{\pi h\phi}} \quad ....(13)$$

and oil in place at the start of the decline analysis is

$$OIP = \frac{V_p\ (1 - s_w)}{(\beta)_{\overline{p}_R}} \quad ....(14)$$

Finally, the original oil in place is determined from

$$OOIP = OIP + N_p \quad ....(15)$$

where N_p is the cumulative production to the start of the decline analysis.

<u>Changes in Backpressure</u>

Since many of the wells in the School Creek Field were evaluated under flowing conditions with more than one change in backpressure occurring, we have extended the single backpressure change superposition equation given in reference 2. Expressed in terms of $m(p)_{oil}$, for simplicity, we have

$$q(t) = \frac{kh\,[m(\overline{p}_R) - m(p_{wf_1})]}{141.2\left[\ln\left(\frac{r_e}{r_w'}\right) - \frac{1}{2}\right]} \Bigg\{ q_{Dd}(t_{Dd}) + \frac{m(p_{wf_1})-m(p_{wf_2})}{m(\overline{p}_R)-m(p_{wf_1})} q_{Dd}(t_{Dd}-t_{Dd_1}) + \frac{m(p_{wf_2})-m(p_{wf_3})}{m(\overline{p}_R)-m(p_{wf_1})}$$

$$\cdot\, q_{Dd}(t_{Dd} - t_{Dd_2}) + \ldots + \frac{m(p_{wf_{n-1}})-m(p_{wf_n})}{m(\overline{p}_R)-(p_{wf_1})}$$

$$\cdot\, q_{Dd}(t_{Dd} - t_{Dd_{n-1}}) \Bigg\} \quad \ldots\ldots\ldots\ldots\ldots\ldots(16)$$

The rate change Δq for any backpressure change is a constant fraction of the initial rate at the same initial transient time period, as the rate change retraces the original q_{Dd} - t_{Dd} curve. The same value of the decline exponent b is used for all rate change superposition calculations.

$$\Delta q_1 = q_2 = q_1\left[\frac{m(p_{wf_1}) - m(p_{wf_2})}{m(\overline{p}_R) - m(p_{wf_1})}\right] \quad \ldots\ldots(17)$$

and $$\Delta q_2 = q_3 = q_1\left[\frac{m(p_{wf_2}) - m(p_{wf_3})}{m(\overline{p}_R) - m(p_{wf_1})}\right] \ldots\ldots.(18)$$

Note that the $q_1/[m(\overline{p}_R) - m(p_{wf1})]$ is the initial productivity index in BOPD/psi or BOPD/psi^2, whichever is appropriate, times a Δp or $\Delta(p^2)$ term for successive flowing pressure changes.

For the more general expression used in this study for pressure above and below the bubble point pressure

$$\Delta q_1 = q_2 = \frac{q_1}{\Delta m(p)_1}\left[\frac{p_{wf_1}^{\,2} - p_{wf_2}^{\,2}}{2p_b}\right] \quad \ldots\ldots.(19)$$

and

$$\Delta q_2 = q_3 = \frac{q_1}{\Delta m(p)_1}\left[\frac{p_{wf_2}^{\,2} - p_{wf_3}^{\,2}}{2p_b}\right] \quad \ldots\ldots(20)$$

where $$\Delta m(p)_1 = (\overline{p}_R - p_b) + \left(\frac{p_b^{\,2} - p_{wf_1}^{\,2}}{2p_b}\right) \ldots\ldots(21)$$

If and when $\overline{p}_R \leq p_b$ the expression reduces to the $\Delta(p^2)$ form. Similarly when $p_{wf} > p_b$ the Δp form is obtained. The Δp form would be appropriate for use with decline exponent values of b = 0 and Δp^2 form for b values greater than zero. For $\Delta(p^2)$, $\overline{p}_R \leq p_b$, the first backpressure change relationship becomes

$$\Delta q_1 = q_2 = \frac{q_1}{(\overline{p}_R^{\,2} - p_{wf_1}^{\,2})} \cdot (p_{wf_1}^{\,2} - p_{wf_2}^{\,2}) \quad \ldots(22)$$

For Δp, $p_{wf} > p_b$, the first backpressure change relationship becomes

$$\Delta q_1 = q_2 = \frac{q_1}{(\overline{p}_R - p_{wf})} \cdot (p_{wf_1} - p_{wf_2}) \quad \ldots\ldots(23)$$

Successive rate changes would be handled as shown in the previously given equations.

One should note that if $(\overline{\mu\beta})$ were correctly evaluated from $m(p)_{oil}$ using the inflow performance relationship discussed in the Appendix, all the decline cline curve analysis could be done directly in pressure terms i.e.

$$(\overline{\mu\beta}) = \frac{\overline{p}_R - p_{wf}}{m(\overline{p}_R) - m(p_{wf})} \quad \ldots\ldots\ldots\ldots\ldots\ldots(24)$$

A detailed example illustrating two backpressure changes is given for the Federal A-1 well, Figures 9 and 10 and Tables 9 and 9A. The example is carried out using the type curve match point and the basic Arps form of the decline equation. The procedure is quite simple using the concept of superposition given by equation 16.

A convenient equation[8] that can be used for calculating the <u>total</u> Δq as a result of n pressure changes is, <u>for</u> a Δp case,

$$p_{wf_n} = p_{wf_1} - \left\{\frac{\overline{p}_R - p_{wf_1}}{q_1}[\Delta q_1 + \Delta q_2 + \ldots + \Delta q_n]\right\} \quad (25)$$

for $m(p)_{oil}$

$$p_{wf_n} = \sqrt{p_{wf_1}^{\,2} - \frac{(2\bar{p}_R\, p_b - p_b^{\,2} - p_{wf_1}^{\,2})(\Delta q_1 + \Delta q_2 + \ldots \Delta q_n)}{q_1}} \qquad \ldots\ldots(26)$$

The Δq values are all specifically defined at a common point in time with respect to the initial rate q_1; 1 day or 1 month, for example. A one month time period is used in this study. The Federal A-1 example illustrates this point. (See Figure 9). One can also back calculate intermediate flowing pressures and rate changes Δq while performance matching knowing the initial flowing pressure and rate, and the final flowing pressure. This also will be discussed with the Federal A-1 example.

METHOD OF DECLINE ANALYSIS

Log-Log Data Plots

The first step in approaching the rate-time log-log analysis in the study of the School Creek Field was to make a log-log plot of all the rate-time data for each well. We next examined each well's plot to find when it actually started on decline. The rate-time data was then reinitialized at the point of decline to t = 0 and a new log-log plot for each well was prepared. We have thus eliminated the constant rate or excess capacity time period which actually represents the constant rate solution instead of the constant wellbore pressure solution. For log-log type curve analysis, we can't do decline analysis until the well is actually on decline.

Based on the assumption that each well was draining its 160 acre spacing and that all wells had been equally stimulated - i.e. r_e/r_w' would then be the same for each well, a School Creek Field Type Curve was constructed by overlaying each well's log-log curve, with the axis all kept parallel, until a single curve was obtained. Figure 5 represents this attempt to obtain a total field type curve using data from 19 wells that exhibited a clear decline in their data. Note the "apparent" long transient period demonstrated by wells D-1, BA-1, and K-3. If this field type curve were valid, we would have a simple and quick method of preparing an oil production forecast and of determining ultimate recoverable reserves for these wells and the remaining completions. We would take the reinitialized log-log plot for each well, find the best match on the field type curve, and draw a line thru the data down the depletion stem of b = 0.30. Future rates would be read directly from the real time plot. Ultimate recovery would then be a summation of forecasted rates plus the cumulative production to the start of decline, plus any additional production as a result of placing the well on pump, where applicable.

To determine if the apparent transient stem was real, wells D-1, BA-1, and K-3 were all evaluated for k and skin (s) from a log-log type curve match on the constant wellbore pressure solution (Figures 2 or 5 of reference 3). The evaluation of the match points lead to unreasonable values of permeability and, more specifically skins for all three wells. None of the wells were massively hydraulically fractured.

Well	k-md	s
D-1	0.017	-7.6
BA-1	0.040	-8.2
K-3	0.024	-8.0

It was therefore concluded that the data for these three wells was not really transient and should be placed in the early depletion period of the total field type curve. Figure 6 is our final School Creek Field Type Curve that does not exhibit a long transient stem. The field type curve is primarily a depletion type curve with a b = 0.30. (We will later discuss the b = 0.30 selected for this study.) Blind matching of log-log data to a type curve and extrapolation can sometimes lead to erroneous production forecasts. An evaluation of the match points to obtain reservoir variables for all wells being studied should give consistent and reasonable numbers when compared with each other thus confirming the validity of the forecast and the ultimate reserves numbers developed. The elimination of the apparent transient stem in this case is a good example of such a checking procedure. The composite type curve, Figure 4 of reference 2, was used for all match point evaluations performed in this study.

Basic Well and Reservoir Data

Table 1 lists basic individual well information and the match points obtained from a log-log type curve evaluation for 40 well completions. Three of the wells are commingled. The table lists first production, the start of decline analysis and the cumulative production to the start of the decline analysis. Initially, virtually all wells came on flowing with several on curtailed or restricted production before starting on decline. Many wells, because of early high gas-oil-ratios and gas disposition problems, were shut in for as much as a year before being returned to production. This accounts for the difference in time of as much as one year between first production and start of decline, with little cumulative production for some wells during this interval.

Reservoir shut-in pressures, $\bar{p}_R$, were generally assumed to be close to the original pressure of approximately 3600 psi except in a few cases where bottomhole pressure surveys were available to indicate otherwise. Flowing pressures were estimated from general pressure surveys conducted on 10 wells in late 1982 and early 1983. Fluid levels shot on pumping wells indicated a minimum bottomhole flowing pressure of approximately 100 psi.

Porosity, thickness and water saturation for each well were furnished by a log analyst. Figure 4 is a permeability-porosity plot developed from 43 plug samples taken on four wells in the field. The core porosities, in general, are significantly less than the average values determined from log analysis. This will be discussed further under calculated r_e values.

The final four columns of the table list the match points obtained from the log-log type curve analysis for each of the well completions in terms of $t - t_{Dd}$ and $q(t) - q_{Dd}$ obtained using the composite type curve (Figure 4 of reference 2) and a decline exponent b = 0.30.

PVT Data

PVT properties required for evaluation of reservoir variables from the type curve match points are presented in Table 2 and also Figure 3. These are μ, β and c_t, all evaluated at reservoir shut-in- pressure, $\overline{p}_R$. The total compressibility term, c_t, was calculated using a water compressibility, c_w, of 3×10^{-6} psi^{-1} and pore volume compressibility, c_f, obtained from Hall's[13] correlation. The product $(\overline{\mu\beta})$ was "mechanically" evaluated at the average pressure $(\overline{p}_R + p_{wf})/2$.

Initially only two PVT samples were available for this study, the Federal EE-1 bottomhole sample to represent Channel Sand completions and the Federal J-1 bottomhole sample to represent Bar Sand completions. The Matheson E-1 PVT surface recombined sample became available only after our initial studies were virtually complete. This sample, because of the vastly different gas-oil-ratio (763 SCF/B versus 1557 SCF/B for the Federal EE-1 well) and because of being a surface recombined sample, had been labeled an unrepresentative sample. Inspection of initial GORs plotted for each well and a gas-oil-ratio versus fractional recovery curve, based on original oil in place developed from the match point evaluations, clearly suggested that the Matheson E-1 sample was valid. The final summary of the evaluation of reservoir variables from type curve analysis was made using the Federal EE-1 PVT data for all wells south of and including wells LL-1, H-1 and R-3. See Figure 1 and Tables 3 and 4. For wells to the north of these wells we used the PVT data from the Matheson E-1 well sample.

Because the study had been virtually completed when the Matheson E-1 sample results became available, we have included the results of all channel sand wells evaluated using both fluid samples. Basic patterns of evaluation results remained essentially the same between the northern and southern wells, i.e., higher percentage recoveries for the southern wells than the northern wells since their actual rate-time performance was based on the real fluid present, not what we selected to use for the final evaluation summary. The more undersaturated a well was, the less recovery would be obtained as compared with a well with a fluid saturated at its initial shut-in pressure, all else being equal. Tables 5, 6, 7, and 8 summarize the results of the match point evaluations based on $(\overline{p}_R - p_{wf})/(\overline{\mu_o\beta})$ and $m(p)_{oil}$ evaluation.

Calculated Results From Decline Curve Analysis

The final results of the type curve evaluation in terms of calculated reservoir variables are presented in Tables 3 and 4; the wells have been arranged on the basis of PVT areas. An $m(p)_{oil}$ evaluation was used for all results given in Table 3 and a $(\overline{p}_R - p_{wf})/(\overline{\mu_o\beta_o})$ evaluation for all values in Table 4.

Pore Volume (V_p)

The pore volume calculations are based on equations 6 and 12, where

$$V_p = \frac{(\overline{\mu\beta})}{(\mu c_t)_{\overline{p}_R}\ (\overline{p}_R - p_{wf_1})} \cdot \frac{t}{t_{Dd}} \cdot \frac{q(t)}{q_{Dd}} \quad .....(6)$$

and

$$V_p = \frac{(\beta)_{\overline{p}_R}}{(c_t)_{\overline{p}_R}\left[(\overline{p}_R - p_{wf}) + \dfrac{(p_b{}^2 - p_{wf_1}{}^2)}{2p_b}\right]} \cdot \frac{t}{t_{Dd}} \cdot \frac{q(t)}{q_{Dd}} \quad (12)$$

Equation 6 would most certainly apply to reservoirs where the single phase liquid solution is applicable, i.e., where the decline curve exponent $b \simeq 0$. The introduction of the $(\overline{\mu\beta})$ term evaluated at $(\overline{p}_R + p_{wf})/2$ with the Δp form is simply an attempt to account for solution-gas drive or two phase flow behavior. A rigorously derived $(\overline{\mu\beta})$ from m(p) concepts, as discussed previously, would be the approach to make equation 6 and 12 equivalent.

For solution gas drive reservoirs, reference 2 demonstrates that the $\Delta(p^2)$ form of IPR (oil well backpressure curve with n = 1.0) used with a nonlinear $\overline{p}_R$ versus N_p material balance relationship produces a decline exponent b = 0.33. Levine and Prats[9], in their simulation study of a solution gas drive reservoir producing under a constant wellbore pressure condition, presented a log q_D - log t_D type curve. (See their Figure 11.) The depletion stem of their type curve basically fits a decline exponent $b \cong 0.33$. Figure 7 illustrates one of several wells in the School Creek Field that exhibited rate-time data in a sufficient stage of decline to help us establish a single decline exponent $b \cong 0.30$. All our decline curve analysis and rate predictions were based on matching and forecasting on b = 0.30 for all wells. All forecasts for this study were done by graphical projection.

Figure 8 is a plot of percent recovery versus bottomhole flowing pressure for the Federal A-1 well. Using equations 6 and 12, the bottomhole flowing pressure was varied between 1600 psi to 100 psi and the pore volume V_p and OOIP calculated. Ultimate recovery was fixed at 36,000 BO for both $\Delta p/(\overline{\mu\beta})$ and $\Delta m(p)_{oil}$ cases to arrive at a percent recovery. Note the lack of sensitivity in percentage recovery for the $\Delta m(p)_{oil}$ case with the variation of bottomhole flowing pressure. Since the $\Delta m(p)_{oil}$ case is effectively a difference in pressures squared effect, we do not see a proportional increase in rate with drawdown as in the $(\overline{\mu\beta})$ case even though $(\overline{\mu\beta})$ was evaluated at each flowing pressure. This is virtually identical with the effect found for gas wells. The precise determination of flowing pressure, p_{wf}, may not then greatly affect our final results.

Oil in Place

Oil in place is calculated directly from V_p using equation 14

$$OIP = \frac{V_p\ (1-s_w)}{(\beta)_{\bar{p}_R}} \quad \text{..............(14)}$$

The calculated oil in place is at the start of decline which, when added to the cumulative production up to the start of the decline analysis, yields the original oil in place, OOIP, equation 15. The original oil in place is later used to calculate fractional oil recoveries, Table 10, and GOR versus fractional recovery, in an attempt to help identify or confirm different fluid properties used in the field analysis and also to possibly identify different rock types.

Calculated Drainage Radius (r_e)

A "calculated" drainage radius is determined from V_p with equation 13

$$r_e = \sqrt{\frac{V_p \times 5.615}{\pi h \phi}} \quad \text{................(13)}$$

The calculated value of r_e is not only a function of pore volume V_p determined from the type curve analysis match point but also of porosity ϕ and thickness h. In this type of reservoir, with indicated thin "dirty" sands and possible limited areal extent, the value of average h used as determined from the logs may be too high. This would result in a calculated r_e value in some cases much less than r_e = 1490 feet for 160 acres. Also, very few of the core sample plugs obtained from wells in the field (see Figure 4) appear to approach the average porosity values reported from the log analysis listed on Table 1. If one were to build a simulation model of the School Creek Field, outlined in Figure 1, based on the log derived values of ϕ, h, and 160 acre spacing for each well, we would have to cut the pore volume to match the type curve analysis derived reservoir variables, specifically oil in place, that have already been history matched to the rate-time decline data.

To come up with calculated values of r_e approaching on average the 160 acre field spacing, the ϕh product would have to be decreased. Otherwise, the rather tenuous conclusion that many wells are not draining the existing spacing could lead to a consideration of infill drilling.

Productivity Factor (P.F.)

The productivity factors for each well are calculated from equations 5 and 11,

$$P.F. = \frac{kh}{\left[\ln\left(\frac{r_e}{r_w'}\right) - \frac{1}{2}\right]} = \frac{141.2\ (\overline{\mu\beta})}{\bar{p}_R - p_{wf_1}} \cdot \frac{q(t)}{q_{Dd}} \quad \text{..(5)}$$

where $(\overline{\mu\beta})$ is evaluated at average pressure $(\bar{p}_R + p_{wf})/2$

and

$$P.F. = \frac{kh}{\left[\ln\left(\frac{r_e}{r_w'}\right) - \frac{1}{2}\right]} = \frac{141.2\ (\mu\beta)_{\bar{p}_R}}{\left[(\bar{p}_R - p_b) + \frac{(p_b^{\ 2} - p_{wf_1}^{\ 2})}{2p_b}\right]} \cdot \frac{q(t)}{q_{Dd}} \quad \text{.........(11)}$$

Since there is a lack of early time transient rate data to sufficiently define an r_e/r_w' stem, unique values of permeability and skin cannot be calculated for each well. We know that all completions were initially stimulated. The core data indicates an arithmetic average permeability of 0.650 md and a geometric average of 0.195 md, with a range of 0.2 md to 7 md. We also had one buildup test conducted on the KK-1 well where the final flowing pressure prior to shut-in was above the bubble point pressure. The analysis yielded a value of k = 2.5 md and s = -3.4.

A range of values of skin from 0 to -4 was selected to evaluate permeabilities for each well. When we fix r_w' on the basis of skin, $r_w' = r_w e^{-s}$, and having previously calculated r_e from the pore volume calculation we can then calculate kh and k from equations 5 and 11.

The ranges of values of k listed on tables 3 and 4 for various values of skin are surprisingly narrow within a given table and even between the two methods of calculation used. It should be pointed out that the values of permeability and skin calculated from the decline curve analysis are those at the start of the decline analysis.

If a good correlation from the core derived ϕ - k plot had been obtained and if log derived average porosities were considered reasonably reliable, we could have used it to determine k and then its corresponding skin from the tables for each well. Based solely on the KK-1 build-up analysis results and the fact that all wells were stimulated, one could also select the -3 skin columns on Table 3 or 4 to arrive at specific values of permeability at the start of decline for each well. There are no unreasonable values of permeabilities listed on either table. Nearly all lie within the range of the core permeabilities shown on Figure 4. Values of permeabilities in the 10s or 100s md on any well would, of course, be suspect.

Example of Effect of Backpressure Change on Recovery and Decline

The equations to calculate the change in producing rates with backpressure changes have been given previously as equations 16 - 26. The Federal A-1 well produced against three different flowing pressures that resulted in two rate changes. Figure 9 is a log-log plot of the rate-time data with the solid line through the points calculated from the type curve match points used with the Arps hyperbolic decline equation. Only the first and last flowing pressures of 1400 psi and 100 psi, respectively, were known. Equation 26, solved in terms of Δq total with p_{wf3} = 100 psi yielded a total Δq = 747 BOPM. A trial and error calculation was then made varying Δq_1 until a best fit of both rate changes was obtained. This resulted in a p_{wf2} = 1069 psi.

Tables 9 and 9-A illustrate in detail the method of developing a forecast with two backpressure changes using the $m(p)_{oil}$ approach. Note specifically that since the rate-time decline is undergoing depletion, the Arps equation is used for all the calculations. One does not have to deal with the reservoir variables, kh, s, r_e/r_w', obtained from the match evaluations. This, however, would not be the case for a transient situation. Theoretically, the rates for the first few months should be calculated at the mid-point of the time interval, i.e., 0.5, 1.5, 2.5, to represent average monthly production rates. For simplicity of presentation of the superposition example, the rates have been evaluated at full month time intervals.

Table 9-A column 2 lists the rates for the initial flowing pressure, p_{wf1}, calculated from Arps' equation with b = 0.3, q_i = 4545.5 BOPM and D_i = 0.212 mo^{-1}. The rate change as a result of a choke change to p_{wf2} = 1069 psi is listed in column 3. It is simply a constant fraction of the initial decline rates. The second backpressure change, when the well was placed on pump to p_{wf3} = 100 psi, is treated similarly. For superposition, columns 3 and 4 are retabulated at a time 1 month past the actual time of the pressure change. Total rate is then the sums of columns 2, 5, and 6. Adding the cumulative production to the start of decline analysis (2633 BO), we have

	N_p Ultimate, BO	
	$\Delta m(p)_{oil}$	$\Delta(p)$
No backpressure change	30,347	30,347
First backpressure change	32,667	34,668
Second backpressure change	35,858	47,226

The Δp numbers in the above table were generated for comparison by recalculating Δq_1 and Δq_2 on the basis of a Δp superposition using equation 23. From this approach, a procedure using actual production data (and its projected rates for a known initial flowing pressure) could be developed to determine the effect of a backpressure change on ultimate recovery, as follows.

Determine N_p at p_{wf1} to t = T, where T = total time of rate-time forecast,

then $$\Delta N_{p_1} = \frac{\Delta q_1}{q_1} \cdot \sum_{t=1}^{T - t\,@\,p_{wf_2}} q \text{ actual}$$

and $$\Delta N_{p_2} = \frac{\Delta q_2}{q_1} \cdot \sum_{t=1}^{T - t\,@\,p_{wf_3}} q \text{ actual}$$

where q actual may also be actual production plus that projected for the initial flowing pressure, p_{wf1}.

$$\text{Ultimate Recoverable} = N_p + \Delta N_{p_1} + \Delta N_{p_2}$$

Similarly, actual early time production rates instead of calculated values can be used to generate the rate-time superposition as illustrated in Table 9-A. This in essence would have the effect of including a downtime if any early time rate variations were due to downtime.

Figure 10 illustrates one more point about backpressure changes with regard to the decline exponent. As has been previously pointed out in references 2 and 3, the sum of two forecasts, both having the same value of decline exponent b, will rarely result in a total forecast having the same decline exponent. In general, the total forecast decline exponent will be larger. Reinitializing the rate-time data after the second backpressure change which also has b = 0.3 resulted in a decline exponent b = 0.40.

Finally, unless all wells are placed on pump at the same time, a backpressure change can cause a well's drainage radius to increase with respect to offset wells. The given superposition example implicitly assumes that r_e remains constant.

Commingled Wells

There are three wells in the School Creek Field where Bar Sand production and Channel Sand production are presently commingled. Figures 11 and 12 for the Federal K-1 well illustrate the method of analysis used to evaluate these wells. A difference curve was developed between the forecast rates of the Channel Sand production only and the commingled production which came on production later. Separate forecasts were then made and added together.

Summary of School Creek Field OOIP and Ultimate Recovery

Table 10 summarizes the results of the calculated original oil in place and ultimate recovery forecast for each well based on an $m(p)_{oil}$ and a $\Delta p/(\overline{\mu\beta})$ evaluation. The superposition of rates as a result of backpressure changes using equations 19 and 23 have also been included where appropriate.

Channel Sand completion results are divided into the northern and southern areas of the field based on the two PVT samples discussed previously. Both evaluation methods indicate a much lower percentage recovery for wells in the northern portion of the field as compared with wells in the southern portion. Wells in the southern portion have percentage recoveries near twice those of wells to the north. This would be consistent solely on the basis of the differences in bubble point pressures between the two fluid samples. Values of percentage recoveries are always lower for the $m(p)_{oil}$ evaluation method. With regard to the additional recoverable reserves that could possibly be obtained by placing all wells on pump to a final bottomhole flowing pressure of 100 psi, the following table summarizes those results. (Nearly half of the wells were initially at or near 100 psi bottomhole flowing pressure at the start of decline.)

	Reserves for Initial Flowing Pressure	Increase of $m(p)_{oil}$ Reserves to p_{wf} of 100 psi		Increase of $\Delta p/(\overline{\mu\beta})$ Reserves to p_{wf} of 100 psi	
	STB	STB	% Increase	STB	% Increase
Northern Wells	223,900	15,594	7%	51,361	23%
Southern Wells	312,105	19,220	6%	67,605	22%
Total Field	819,484	68,354	8%	230,346	28%

If, in fact, the inflow performance relationship based on Δp^2 applies, the percentage increase as a result of placing all wells on pump to a final flowing pressure of 100 psi would be approximately 8% or 68,000 BO. If the inflow performance relationship were to follow a Δp (PI) behavior, the anticipated increase in reserves would be 28% or 230,000 BO. Perhaps the real increase in reserves due to lowering the final bottomhole flowing pressure lies somewhere between these two limits.

Individual Well Gas-Oil-Ratio Performance

Figures 13 thru 16 reflect gas-oil-ratio performance of individual wells in the field based on expressing the recovery factor in terms of each well's actual cumulative production divided by the OOIP calculated from the $m(p)_{oil}$ evaluation. Either method of calculating OOIP should show similar trends. Gas and oil rates are metered separately for each well and are not based on allocation from tests.

Figures 13 and 14 are on an expanded gas-oil-ratio scale in an attempt to help identify rock types in each area of the field. If one assumes the fluids are the same for each area, three different rock types and/or initial water saturations are possibly indicated in the southern portion of the field.

Figures 15 and 16, prepared on a scale where the entire gas-oil-ratio performance of each well can be shown clearly, indicate two different fluids, based mainly on the wells' peak gas-oil-ratio alone which is not a function of the method of calculating an OOIP number. Note that the gas-oil-ratio has turned over on several wells. The peak gas-oil-ratios for the northern wells is generally much lower than those of the southern wells. These gas-oil-ratio curves could be used in developing a gas forecast to go with the oil rate forecast developed from the decline curve analysis.

CONCLUSIONS

Original oil in place values can be calculated from rate-time analysis for individual wells and can also be used with reserves projections developed from the decline analysis to obtain fractional recoveries for each well in a field. These fractional recovery numbers should be reasonable, considering the fluid type and the permeability of the reservoir.

Each well's evaluation of the reservoir variables k, s (skin), OOIP and fractional recovery, obtained from individual well rate-time decline analysis, should give consistent and reasonable numbers when compared with other wells in the field. A single well analysis can give results that are not recognized as being invalid unless compared with other wells in the field.

Failure to consider a future lowering of a well's flowing bottomhole pressure from that causing a well's initial rate-time decline can result in underestimating ultimate recoverable reserves.

A method of treating future backpressure changes based on the superposition principle and an oil well inflow performance relationship is easily applied to decline curve analysis. An oil well inflow performance relationship can be utilized over an entire production forecast, not only at an instant in time.

NOMENCLATURE

- b = reciprocal of decline curve exponent (1/b)
- β = formation volume factor, res vol/surface vol
- c_f = effective rock compressibility, psi^{-1}
- $\bar{c}_t$ = total compressibility, psi^{-1}
- c_w = water compressibility, psi^{-1}
- D_i = initial decline rate, t^{-1}
- e = natural logarithm base 2.71828
- h = thickness, ft
- k = effective permeability, md
- k_{ro} = relative permeability to oil, fraction
- $m(p)_{oil}$ = oil pseudo pressure, psi/cp
- n = exponent of backpressure curve
- N_p = cumulative oil production, STB
- OIP = oil in place at start of decline analysis, STB
- OOIP = original oil in place, STB
- p_b = bubble point pressure, psia
- $\bar{p}_R$ = reservoir shut-in pressure, at start of decline, psia
- p_{wf} = bottomhole flowing pressure, psia
- q_{Dd} = decline curve dimensionless rate
- $q(t)$ = surface rate of flow at time t
- r_e = external boundary radius, ft
- r_w = wellbore radius, ft
- r_w' = effective wellbore radius, ft
- s = skin factor, dimensionless
- S_w = water saturation
- t = time, mo.
- t_{Dd} = decline curve dimensionless time
- T = total time of forecast, mo.
- V_p = reservoir pore volume, ft^3
- μ = viscosity, cp
- ϕ = porosity, fraction of bulk volume

ACKNOWLEDGEMENTS

We wish to thank Phillips Petroleum Company for permission to publish this paper. We also wish to thank U. G. Kiesow, M. D. Bradley, and S. D. Dunstan for their timely assistance in parts of this study.

REFERENCES

1. Arps, J. J.: "Analysis of Decline Curves," TRANS, AIME (1945) 160, 228-247.
2. Fetkovich, M. J.: "Decline Curve Analysis Using Type Curves," J. Pet. Tech (June 1980) 1065-1077.
3. Fetkovich, M. J. , Vienot, M. E., Bradley, M. D., and Kiesow, U. G.: "Decline Curve Analysis Using Type Curves: Case Histories," paper SPE 13169 presented at the 59th Annual Fall Meeting of SPE of AIME, Houston, Texas, September 1984.
4. Carter, R. D.: "Characteristic Behavior of Finite Radial and Linear Gas Flow Systems - Constant Terminal Pressure Case," SPE/DOE 9887 presented at the 1981 SPE/DOE Low Permeability Symposium, Denver, CO, May 27-29, 1981.
5. Carter, R. D.: "Type Curves for Finite Radial and Linear Gas-Flow Systems: Constant Terminal Pressure Case," SPE 12917 presented at the 1984 Rocky Mountain Regional Meeting, Casper, WY, May 1984.
6. Da Prat, Giovanni, Cinco-Ley, Heber and Ramey, H. J., Jr.: "Decline Curve Analysis Using Type Curves for Two-Porosity Systems," Soc. Pet. Eng. J (June 1981) 354-362.
7. Fetkovich, M. J. and Vienot, M. E.: "Shape Factor, C_A, Expressed as a Skin, S_{C_A}," J. Pet. Tech. (February 1985) 321-322.
8. Bradley, M. D.: Personal communication.
9. Levine, J. S. and Prats, M.: "The Calculated Performance of Solution Gas Drive Reservoirs," Soc. Pet. Eng. J. (Sept. 1961) 145-152.
10. Fetkovich, M. J.: "The Isochronal Testing of Oil Wells," paper SPE 4529 presented at the 48th Annual Fall Meeting, Las Vegas, Nev., Sept. 30 - October 3, 1973. (SPE Reprint Series No. 14,265.)
11. Vogel, J. V.: "Inflow Performance Relationships for Solution Gas Drive Wells," J. Pet. Tech. (Jan. 1968), 83.
12. Whitson, C. H.: "Reservoir Well Performance and Predicting Deliverability," Unsolicited paper SPE 12518, U. of Trondheim.
13. Craft, B. C. and Hawkins, M. F., Jr.: "Applied Petroleum Reservoir Engineering, Prentice Hall, Inc. Englewood Cliffs, N.J. (1959) 132.

SI METRIC CONVERSION FACTORS

acre	x 4.046873	E+03	=	m^2
bbl	x 1.589873	E-01	=	m^3
bbl/D	x 1.589873	E-01	=	m^3/D
cp	x 1.0*	E-03	=	Pa•3
ft	x 3.048*	E-01	=	m
ft^3/D	x 2.831685	E-02	=	M^3/D
md	x 9.869233	E-04	=	μm^2
psi	x 6.894757	E-03	=	MPa

*conversion factor is exact

APPENDIX

Oil Pseudo Pressure, $m(p)_{oil}$ For Decline Curve Analysis

Reference 10) introduced the concept of a pseudo-pressure m(p) for oil well drawdown tests similar to that now commonly used for gas wells. It was presented along with a general inflow performance relationship developed from multi-point test data of some 40 oil well tests.

A general inflow performance equation for decline analysis that treats flow both above and below the bubble point pressure for an undersaturated oil well assuming no non-Darcy flow component is

$$q_o = J^* (\bar{p}_R - p_b) + J' \ (p_b{}^2 - p_{wf}{}^2) \quad \text{........(A-1)}$$

$$\text{where } J^* = \frac{kh}{141.2\left[\ln\left(\frac{r_e}{r_w'}\right) - \frac{1}{2}\right]} \cdot \left(\frac{k_{ro}}{\mu_o\beta_o}\right)_{\bar{p}_R} \quad \text{...(A-2)}$$

$$\text{and } J' = J^* (\mu_o\beta_o)_{\bar{p}_R,\, p_b} \cdot \frac{a_2}{2} \quad \text{........(A-3)}$$

Assuming $(\mu_o\beta_o)$ is a constant value above the bubble point pressure equal to $(\mu_o\beta_o)_b$ (the basis for the constant PI assumption for flow above the bubble point pressure, p_b) then (See also Appendix of reference 10)

$$a_2 = \frac{1}{p_b(\mu_o\beta_o)_{p_b}} \quad \text{...............(A-4)}$$

For $1/\mu_o\beta_o$ to go through a zero intercept on draw-down, we are really looking at a $(k_{ro})_{p_{wf}} / (\mu_o\beta_o)$, a pseudo $(\mu_o\beta_o)$. This then would reproduce field data log-log IPR curves with n = 1.00 and also Vogel's[11] Figure 7, a computer generated IPR. (Figure 17 in this paper.)

Thus

$$J' = \frac{J^* \,(\mu_o\beta_o)_{p_b}}{2p_b\,(\mu_o\beta_o)_{p_b}} = \frac{J^*}{2p_b} \qquad \text{.........(A-5)}$$

Substituting equation (A-5) into (A-1) we obtain the final form of the single phase and two phase IPR equation

$$q_o = J^* \left[\frac{(\overline{p}_R - p_b)}{} + \frac{(p_b^{\,2} - p_{wf}^{\,2})}{2p_b} \right] \qquad \text{........(A-6)}$$

or in terms of reservoir variables, with $k_{ro} \equiv 1$ at start of decline analysis

$$q_o = \frac{kh}{141.2\left[\ln\left(\frac{r_e}{r_w'}\right) - \frac{1}{2}\right]} \cdot \frac{1}{(\mu_o\beta_o)_{\overline{p}_R}} \left[(\overline{p}_R - p_b) + \frac{(p_b^{\,2} - p_{wf}^{\,2})}{2p_b} \right]$$

$$\text{............(A-7)}$$

or in terms of $m(p)_{oil}$

$$q_o = \frac{kh}{141.2\left[\ln\left(\frac{r_e}{r_w'}\right) - \frac{1}{2}\right]} \cdot \left[m(\overline{p}_R) - m(p_{wf}) \right] \qquad \text{..(A-8)}$$

For the case of $\overline{p}_R \leq p_b$ we have from equation (A-7)

$$q_o = \frac{kh}{141.2\left[\ln\left(\frac{r_e}{r_w'}\right) - \frac{1}{2}\right]} \cdot \frac{1}{(\mu_o\beta_o)_{\overline{p}_R}} \cdot \frac{(\overline{p}_R^{\,2} - p_{wf}^{\,2})}{2\overline{p}_R}$$

$$\text{.......(A-9)}$$

With $p_R \leq p_b$ we can compare the Vogel and the Δp^2 inflow relationship in terms of $m(p)_{oil}$. We have

$$\Delta p^2 \text{ form} : m(p)_{oil} = \frac{1}{2\overline{p}_R} \cdot \left(\frac{k_{ro}}{\mu_o\beta_o}\right)_{\overline{p}_R} \cdot p^2 \qquad \text{..(A-10)}$$

$$\text{Vogel form}^{12} : m(p)_{oil} = \frac{1}{9}\left(\frac{k_{ro}}{\mu_o\beta_o}\right)_{\overline{p}_R} \cdot \left(p + \frac{4p^2}{\overline{p}_R}\right)$$

$$\text{............(A-11)}$$

The Vogel form would be extremely cumbersome if entered into the constant wellbore pressure solutions as an $m(p)_{oil}$ expression whereas the Δp^2 form results in a simple expression identical in form to the low pressure gas well backpressure equation. Oil well IPR curves, just as gas well backpressure curves are most applicable to the constant wellbore pressure solution conditions. A comparison of the Δp^2 form of IPR and Vogel's IPR equation (both these forms assume a non-Darcy flow component of zero) can be seen in figure 17. The results shown on Vogel's figure 7 are the only complete set of curves given in his paper with which we could make a comparison of the two methods when using the same match point. Vogel's points of match A thru H were used to develop the comparison. Note from the figure 17 comparison that the Δp^2 form of the equation better fits his computer calculated IPR over the entire range of depletion than his own dimensionless form of the IPR equation. At very low flowing pressures approaching 0 flowing pressure, a region we seldom deal with, the Δp^2 form is slightly less than the simulation run result but still closer than using Vogel's dimensionless equation.

Reference 2 illustrates that when the Δp^2 form of the IPR equation is combined with a non-linear p versus N_p relationship for solution gas drive reservoirs, the expected decline curve exponent b = 0.333. This is practically the same value as that found and used in this study.

TABLE 1

SCHOOL CREEK FIELD, CAMPBELL - CONVERSE CO., WYOMING
BASIC RESERVOIR DATA AND DECLINE CURVE MATCH POINTS

Well	Date (Mo - Yr) First Production	Date (Mo - Yr) Start of Decline Analysis	Well Status Pump or Flow	Well Status Date on Pump	N_p to Decline STB	$\bar{p}_R$ psia	p_{wf} psia	Log Data ϕ Fraction	Log Data h Feet	Log Data $(1-S_w)$ Fraction	Match Point w/ (b=0.30) t mo	t_{Dd}	q(t) BOPM	q_{Dd}
A-1	6-81	9-81	F	12-83	2633	3500	1400	.137	9	.70	1	0.212	1000	0.220
C-1	6-81	10-81	P	8-81	6226	3600	100	.138	15	.60	1	0.058	1000	0.680
D-2	1-83	1-83	P	3-82	0	3600	500	.161	7	.52	1	0.156	10	0.110
DD-1	6-82	3-83	F		7828	2900	600	.103	8	.60	1	0.354	1000	0.590
EE-1	5-82	3-83	F		13839	3000	1000	.134	12	.50	1	0.313	1000	0.432
F-1	10-83	10-83	P	6-83	0	3600	100	.100	11	.30	1	0.210	10	0.076
FF-1	4-82	10-83	F		7642	3300	800	.145	10	.70	1	0.510	100	0.086
G-1	6-82	7-82	P	11-83	289	3500	2000	.160	10	.60	1	0.100	100	0.270
GG-1	6-82	9-82	F		3582	3600	1000	.120	5	.60	1	0.130	1000	0.430
GG-2	6-82	6-82	P	11-83	0	3600	400	.125	14	.60	1	0.098	1000	0.914
H-1	10-81	10-81	P	10-81	0	3600	100	.165	8	.60	1	0.083	1000	0.670
I-1	9-81	9-82	F		3839	2900	700	.158	14	.70	1	0.290	1000	0.190
J-1 (B)	5-82	5-83	F	9-83	1761	3600	1400	.240	17	.85	1	0.146	1000	0.205
JJ-1	8-82	8-83	F		4287	3100	600	.149	13	.75	1	0.115	100	0.150
K-1	5-82	6-82	F		501	3600	1000	.134	3.5	.60	1	0.075	1000	0.580
K-1 (B)	3-83	3-83	F		0	3600	1000	.240	5	.90	1	0.185	1000	0.278
K-4	5-82	12-82	P	12-82	7460	3300	100	.150	10	.60	1	0.210	1000	0.417
KK-1	8-82	5-83	F		3643	3300	2000	.130	4	.50	1	0.229	1000	0.527
KK-2	8-82	7-83	P	7-83	1535	3600	100	.140	38	.70	1	0.190	100	0.098
LL-1	8-82	5-83	P	3-83	1468	3600	100	.132	10	.65	10	0.079	10	0.550
LL-2 (B)	8-82	6-83	F		3327	3600	1000	.170	4	.70	1	0.250	100	0.098
O-1	11-81	4-82	F		21473	3600	1600	.148	11	.75	1	0.178	1000	0.231
Q-1	1-83	6-83	P	6-83	689	3600	100	.140	10	.50	1	0.144	100	0.310
R-1	8-82	8-83	P	6-83	1635	3600	100	.123	6	.60	1	0.130	100	0.380
R-2	9-82	8-83	P	3-83	1169	3600	100	.120	10	.60	1	0.092	100	0.670
R-3	7-82	12-82	F		5443	3600	1000	.150	7	.60	1	0.063	1000	0.285
R-3 (B)	5-83	5-83	F		0	3600	1000	.200	15	.90	1	0.115	100	0.047
R-4	4-82	5-83	F		12237	3500	1200	.132	10	.60	1	0.118	100	0.070
S-1	4-82	5-82	F		24533	3600	1000	.150	12	.70	1	0.115	1000	0.264
S-1 (B)	5-83	5-83	F		0	3400	1200	.210	18	.85	1	0.205	1000	0.200
T-1	3-82	6-83	F		23195	3300	1000	.142	20	.75	1	0.280	100	0.069
T-2	5-82	8-83	F		8146	3300	1000	.158	15	.80	1	0.270	100	0.250
T-3	5-82	7-83	P	7-83	1383	3600	100	.153	8	.75	1	0.200	100	0.280
T-4	7-82	5-83	F		7692	3300	1200	.138	14	.55	1	0.239	100	0.201
T-5	2-83	4-83	P	4-83	245	3600	100	.134	11	.65	1	0.300	100	0.088
Ford A-1	6-82	7-82	F		1871	3600	1300	.143	15	.60	1	0.165	1000	0.330
Ford B-1	9-82	2-83	P	11-82	319	3600	100	.152	17	.70	1	0.078	100	0.170
Math B-1	10-80	10-81	P	10-80	10776	3300	100	.160	7	.52	1	0.0713	100	0.131
Math D-1	5-82	5-82	P	3-82	0	3300	600	.143	5	.70	1	0.100	100	0.240
Math E-1	7-81	12-81	P	12-82	7860	3500	1000	.152	16	.60	1	0.111	1000	0.188

TABLE 2

SCHOOL CREEK FIELD, CAMPBELL - CONVERSE CO., WYOMING

Well	Channel Sand PVT Data: Federal EE-1 PVT (p_b = 3400) @ $\bar{p}_R$ μ_o cps	@ $\bar{p}_R$ B_o RB/STB	@ $\bar{p}$ avg. $(\mu_o B_o)$ cps-RB/STB	@ $\bar{p}_R$ c_t x 10^{-6} psi-1	Matheson E-1 PVT (p_b = 2705) @ $\bar{p}_R$ μ_o cps	@ $\bar{p}_R$ B_o RB/STB	@ $\bar{p}$ avg. $(\mu_o B_o)$ cps-RB/STB	@ $\bar{p}_R$ c_t x 10^{-6} psi-1	Bar Sand PVT Data: Federal J-1 PVT (p_b = 2853) @ $\bar{p}_R$ μ_o cps	@ $\bar{p}_R$ B_o RB/STB	@ $\bar{p}$ avg. $(\mu_o B_o)$ cps-RB/STB	@ $\bar{p}_R$ c_t x 10^{-6} psi-1
A-1	0.150	1.90	0.366	27.4	0.46	1.47	0.647	15.7				
C-1	0.150	1.90	0.420	24.6	0.46	1.47	0.696	14.5				
D-2	0.150	1.90	0.400	22.1	0.46	1.47	0.677	13.2				
DD-1	0.200	1.70	0.431	24.5	0.43	1.48	0.707	15.0				
EE-1	0.200	1.70	0.405	21.6	0.44	1.48	0.682	13.4				
F-1	0.150	1.90	0.420	15.9	0.46	1.47	0.696	11.6				
FF-1	0.180	1.70	0.400	27.4	0.45	1.47	0.677	15.6				
G-1	0.150	1.90	0.344	24.5	0.46	1.47	0.638	14.2				
GG-1	0.150	1.90	0.378	24.5	0.46	1.47	0.658	14.7				
GG-2	0.150	1.90	0.405	24.5	0.46	1.47	0.682	14.7				
H-1	0.150	1.90	0.420	24.5	0.46	1.47	0.696	14.1				
I-1	0.200	1.70	0.425	27.5	0.43	1.48	0.702	15.5				
J-1 (B)									0.20	1.70	0.355	25.9
JJ-1	0.180	1.73	0.420	28.9	0.44	1.48	0.696	16.2				
K-1	0.150	1.90	0.378	24.5	0.46	1.47	0.658	14.5				
K-1 (B)									0.20	1.70	0.368	26.9
K-4	0.155	1.88	0.447	24.5	0.45	1.47	0.712	14.3				
KK-1	0.158	1.89	0.351	21.6	0.45	1.89	0.638	13.3				
KK-2	0.150	1.90	0.420	27.5	0.46	1.47	0.696	20.8				
LL-1	0.150	1.90	0.420	26.0	0.46	1.47	0.696	15.2				
LL-2 (B)									0.20	1.70	0.368	22.5
O-1	0.150	1.90	0.355	28.9	0.46	1.47	0.640	16.2				
Q-1	0.150	1.90	0.420	21.7	0.46	1.47	0.696	13.2				
R-1	0.150	1.90	0.420	24.6	0.46	1.47	0.696	14.7				
R-2	0.150	1.90	0.420	24.6	0.46	1.47	0.696	14.7				
R-3	0.150	1.90	0.378	24.5	0.46	1.47	0.658	14.3				
R-3 (B)									0.20	1.70	0.368	26.9
R-4	0.150	1.90	0.374	24.3	0.46	1.47	0.655	14.5				
S-1	0.150	1.90	0.378	27.4	0.46	1.47	0.658	15.5				
S-1 (B)									0.20	1.70	0.368	25.9
T-1	0.180	1.70	0.391	28.9	0.45	1.47	0.670	16.3				
T-2	0.180	1.72	0.391	30.4	0.45	1.47	0.670	16.7				
T-3	0.150	1.72	0.420	29.0	0.46	1.47	0.696	16.0				
T-4	0.180	1.90	0.382	23.2	0.45	1.47	0.672	13.9				
T-5	0.150	1.72	0.420	26.0	0.46	1.47	0.696	15.3				
Ford A-1	0.150	1.90	0.367	24.5	0.46	1.47	0.647	14.4				
Ford B-1	0.150	1.90	0.420	27.4	0.46	1.47	0.696	15.4				
Math B-1	0.158	1.88	0.437	22.1	0.45	1.47	0.712	13.1				
Math D-1	0.150	1.90	0.410	27.4	0.45	1.47	0.686	15.6				
Math E-1	0.150	1.90	0.382	24.4	0.46	1.47	0.672	14.2				

TABLE 3

SCHOOL CREEK FIELD - CALCULATED DECLINE CURVE ANALYSIS RESULTS
$m(p)_{oil}$ EVALUATION

Well	Pore Vol. V_p RB	Start of Decline OIP STB	OOIP STB	Calculated r_e feet	Prod. Factor $\frac{kh}{\ln \frac{r_e}{r_w'} - \frac{1}{2}}$	s = 0 r_w' = .328 k-md	s = -1 r_w' = .892 k-md	s = -2 r_w' = 2.424 k-md	s = -3 r_w' = 6.588 k-md	s = -4 r_w' = 17.90 k-md	
A-1	1104447	525927	528560	1265	7.8542	6.77	5.90	5.02	4.15	3.28	Channel Sand Matheson E-1 PVT
C-1	1144643	467201	473427	994	2.0567	1.03	0.89	0.76	0.62	0.48	
D-2	29481	10429	10429	216	0.1297	0.11	0.09	0.07	0.06	0.04	
F-1	35358	7216	7216	240	0.1840	0.10	0.09	0.07	0.05	0.04	
G-1	272285	111137	111426	552	0.8261	0.57	0.49	0.41	0.32	0.24	
JJ-1	315066	159662	163949	539	1.1995	0.64	0.54	0.45	0.36	0.27	
K-1	1486687	606811	607312	2380	2.6253	6.29	5.54	4.79	4.04	3.29	
K-4	603338	246261	253721	848	3.7869	2.79	2.41	2.03	1.65	1.27	
Q-1	111090	37786	38475	377	0.4511	0.30	0.25	0.21	0.16	0.11	
R-1	90143	36793	38428	467	0.3680	0.41	0.35	0.29	0.23	0.17	
R-2	72243	29487	30656	328	0.2087	0.13	0.11	0.09	0.07	0.05	
Ford A-1	968836	395443	397314	898	4.9183	2.43	2.10	1.78	1.45	1.12	
Ford B-1	320561	152648	152967	471	0.8227	0.33	0.28	0.23	0.18	0.13	
Math B-1	617476	218427	229203	993	1.2054	1.29	1.12	0.95	0.78	0.61	
Math D-1	208739	99399	99399	722	0.6806	0.98	0.84	0.71	0.57	0.44	
Math E-1	2550551	1041041	1048901	1369	8.5120	4.17	3.64	3.11	2.57	2.04	
DD-1	239364	84482	92310	721	1.9285	1.73	1.49	1.25	1.01	0.77	Channel Sand Federal EE-1 PVT
EE-1	436544	128395	142234	697	2.7416	1.64	1.41	1.18	0.95	0.72	
FF-1	91086	37506	45148	335	1.0641	0.68	0.58	0.47	0.36	0.26	
GG-1	791422	249923	253505	1535	1.7561	2.79	2.44	2.09	1.74	1.39	
GG-2	461396	145704	145704	686	0.7718	0.39	0.34	0.28	0.23	0.17	
H-1	734543	231961	231961	997	1.0406	0.98	0.85	0.72	0.59	0.46	
I-1	821613	338311	342150	815	6.0868	3.18	2.75	2.31	1.88	1.44	
KK-1	694523	183736	187379	1545	2.5211	5.02	4.38	3.75	3.12	2.49	
KK-2	195445	72006	73541	256	0.7114	0.12	0.10	0.08	0.06	0.04	
LL-1	72149	24682	26150	313	0.0126	0.01	0.01	0.01	.01	.01	
O-1	1049477	414267	435740	1073	3.7613	2.60	2.25	1.91	1.57	1.23	
R-3	2463966	778095	783538	2048	2.6496	3.12	2.74	2.36	1.98	1.60	
R-4	374090	118134	130371	712	1.1906	0.86	0.74	0.62	0.50	0.38	
S-1	1302969	480041	504574	1137	2.8604	1.82	1.59	1.35	1.11	0.87	
T-1	205575	89640	112835	360	1.3907	0.45	0.38	0.31	0.24	0.17	
T-2	55937	26017	34163	205	0.3838	0.15	0.13	0.10	0.08	0.05	
T-3	67939	26818	28201	315	0.2745	0.22	0.18	0.15	0.12	0.08	
T-4	107785	34466	42158	316	0.4996	0.23	0.19	0.16	0.12	0.08	
T-5	145800	49879	50124	420	0.7923	0.48	0.41	0.34	0.26	0.19	
J-1 (B)	1198370	599185	600946	725	4.2095	1.78	1.54	1.29	1.04	0.79	Bar Sand PVT
K-1 (B)	614938	325555	325555	957	2.8428	4.25	3.68	3.11	2.55	1.98	
LL-2 (B)	154330	63548	66875	637	0.8064	1.43	1.22	1.02	0.82	0.62	
R-3 (B)	585130	309774	309774	590	1.6814	0.78	0.67	0.56	0.45	0.34	
S-1 (B)	930145	465072	465072	663	4.5877	1.81	1.56	1.30	1.05	0.79	

TABLE 4

SCHOOL CREEK FIELD - CALCULATED DECLINE CURVE ANALYSIS RESULTS
$(\bar{p}_R - p_{wf})/\overline{\mu_o B_o}$ EVALUATION

Well	Pore Vol. V_p RB	Start of Decline OIP STB	OOIP STB	Calculated r_e feet	Prod. Factor $\frac{kh}{\ln \frac{r_e}{r_w'} - \frac{1}{2}}$	s = 0 r_w' = .328 k-md	s = -1 r_w' = .892 k-md	s = -2 r_w' = 2.424 k-md	s = -3 r_w' = 6.588 k-md	s = -4 r_w' = 17.90 k-md	
A-1	898346	427784	430417	1141	6.3885	5.43	4.72	4.01	3.30	2.59	Channel Sand Matheson E-1 PVT
C-1	755925	308541	314767	807	1.3583	0.66	0.57	0.48	0.39	0.30	
D-2	20959	7414	7414	182	0.0922	0.08	0.06	0.05	0.04	0.02	
F-1	23350	4765	4765	194	0.1215	0.07	0.05	0.04	0.03	0.02	
G-1	241168	98436	98725	519	0.7317	0.50	0.43	0.36	0.28	0.21	
JJ-1	226419	114739	119026	457	0.8621	0.45	0.38	0.31	0.25	0.18	
K-1	1147688	468444	468945	2091	2.0267	4.78	4.20	3.62	3.05	2.47	
K-4	394845	161161	168621	685	2.4783	1.77	1.52	1.28	1.03	0.78	
Q-1	73364	24954	25643	306	0.2979	0.19	0.16	0.13	0.10	0.07	
R-1	59530	24298	25933	379	0.2431	0.27	0.22	0.18	0.14	0.10	
R-2	47709	19473	20642	266	0.1379	0.09	0.07	0.06	0.04	0.03	
Ford A-1	779935	318341	320212	806	3.9593	1.93	1.66	1.40	1.14	0.87	
Ford B-1	211699	100809	101128	382	0.5433	0.21	0.18	0.15	0.11	0.08	
Math B-1	404097	142946	153722	803	0.7889	0.82	0.71	0.60	0.48	0.37	
Math D-1	150804	71811	71811	613	0.4917	0.69	0.59	0.50	0.40	0.30	
Math E-1	1989906	812207	820067	1209	6.6410	3.20	2.79	2.37	1.96	1.54	
DD-1	183104	64625	72453	630	1.4752	1.30	1.12	0.93	0.75	0.56	Channel Sand Federal EE-1 PVT
EE-1	346668	101961	115800	620	2.1772	1.28	1.10	0.92	0.73	0.55	
FF-1	73965	30456	38098	301	0.8641	0.55	0.46	0.37	0.29	0.20	
GG-1	707700	223484	227066	1451	1.5704	2.48	2.17	1.85	1.54	1.22	
GG-2	384481	121415	121415	626	0.6432	0.32	0.28	0.23	0.19	0.14	
H-1	587180	185425	185425	891	0.8319	0.77	0.67	0.56	0.46	0.35	
I-1	637459	262483	266322	717	4.7225	2.43	2.09	1.75	1.41	1.08	
KK-1	655552	173426	177069	1501	2.3797	4.72	4.12	3.53	2.93	2.34	
KK-2	156235	57560	59095	229	0.5687	0.09	0.08	0.06	0.05	0.03	
LL-1	57674	19731	21199	279	0.0101	0.01	0.01	.01	.01	.01	
O-1	995812	393084	414557	1045	3.5690	2.46	2.13	1.81	1.48	1.16	
R-3	2142759	874595	880038	1909	4.1245	4.81	4.22	3.64	3.05	2.46	
R-4	338993	107050	119287	677	1.0790	0.77	0.66	0.55	0.45	0.34	
S-1	1169126	556727	581260	1077	4.4526	2.82	2.45	2.08	1.71	1.33	
T-1	169150	73757	96952	326	1.1444	0.37	0.31	0.25	0.19	0.14	
T-2	46026	21407	29553	186	0.3158	0.12	0.10	0.08	0.06	0.04	
T-3	68966	27223	28606	317	0.2787	0.22	0.19	0.15	0.12	0.08	
T-4	90675	28995	36687	289	0.4203	0.19	0.16	0.13	0.10	0.07	
T-5	116550	39872	40117	375	0.6334	0.38	0.32	0.26	0.20	0.15	
J-1 (B)	1040805	520402	522163	675	3.6561	1.53	1.32	1.10	0.89	0.67	Bar Sand PVT
K-1 (B)	511535	270813	270813	872	2.3648	3.49	3.02	2.55	2.07	1.60	
LL-2 (B)	128380	52862	56189	580	0.6708	1.17	1.00	0.84	0.67	0.50	
R-3 (B)	486739	257686	257686	538	1.3987	0.64	0.55	0.46	0.36	0.27	
S-1 (B)	787611	393805	393805	610	3.8847	1.52	1.30	1.09	0.87	0.65	

SPE 14737

TABLE 5

SCHOOL CREEK FIELD - CALCULATED DECLINE CURVE ANALYSIS RESULTS
BASED ON FEDERAL EE-1 (CHANNEL SAND) AND $m(p)_{oil}$ EVALUATION

Well	Pore Vol. V_p RB	Start of Decline OIP STB	OOIP STB	Calculated r_e feet	Prod. Factor $\frac{kh}{\ln \frac{r_e}{r_w} - \frac{1}{2}}$	s = 0 r_w' = .328 k-md	s = -1 r_w' = .892 k-md	s = -2 r_w' = 2.424 k-md	s = -3 r_w = 6.588 k-md	s = -4 r_w' = 17.90 k-md
A-1	965906	355860	358493	1183	3.9091	3.34	2.91	2.47	2.04	1.60
C-1	1031488	325733	331959	944	1.0253	0.51	0.44	0.37	0.31	0.24
D-2	26889	7359	7359	207	0.0645	0.05	0.05	0.04	0.03	0.02
DD-1	239364	84482	92310	721	1.9285	1.73	1.49	1.25	1.01	0.77
EE-1	436544	128395	142234	697	2.7416	1.64	1.41	1.18	0.95	0.72
F-1	39437	6227	6227	253	0.0917	0.05	0.04	0.03	0.03	0.02
FF-1	91086	37506	45148	335	1.0641	0.68	0.58	0.47	0.36	0.26
G-1	237031	74852	75141	515	0.4046	0.28	0.24	0.20	0.16	0.12
GG-1	791422	249923	253505	1535	1.7561	2.79	2.44	2.09	1.74	1.39
GG-2	461396	145704	145704	686	0.7718	0.39	0.34	0.28	0.23	0.17
H-1	734543	231961	231961	997	1.0406	0.98	0.85	0.72	0.59	0.46
I-1	821613	338311	342150	815	6.0868	3.18	2.75	2.31	1.88	1.44
J-1 (B)	1198370	599185	600946	725	4.2095	1.78	1.54	1.29	1.04	0.79
JJ-1	232600	100838	105125	463	0.6463	0.34	0.29	0.24	0.19	0.14
K-1	1338189	422586	423087	2258	1.3020	3.10	2.73	2.36	1.99	1.61
K-1 (B)	614938	325555	325555	957	2.8428	4.25	3.68	3.11	2.55	1.98
K-4	531559	169646	177106	796	1.9689	1.44	1.24	1.04	0.85	0.65
KK-1	694523	183736	187379	1545	2.5211	5.02	4.38	3.75	3.12	2.49
KK-2	195445	72006	73541	256	0.7114	0.12	0.10	0.08	0.06	0.04
LL-1	72149	24682	26150	313	0.0126	0.01	0.01	0.01	.00	.00
LL-2 (B)	154330	63548	66875	637	0.8064	1.43	1.22	1.02	0.82	0.62
O-1	1049477	414267	435740	1073	3.7613	2.60	2.25	1.91	1.57	1.23
Q-1	103312	27187	27876	363	0.2249	0.15	0.12	0.10	0.08	0.06
R-1	82352	26006	27641	447	0.1834	0.21	0.17	0.14	0.11	0.08
R-2	65999	20842	22011	314	0.1040	0.07	0.06	0.05	0.03	0.02
R-3	2463966	778095	783538	2048	2.6496	3.12	2.74	2.36	1.98	1.60
R-3 (B)	585130	309774	309774	590	1.6814	0.78	0.67	0.56	0.45	0.34
R-4	374090	118134	130371	712	1.1906	0.86	0.74	0.62	0.50	0.38
S-1	1302969	480041	504574	1137	2.8604	1.82	1.59	1.35	1.11	0.87
S-1 (B)	930145	465072	465072	663	4.5877	1.81	1.56	1.30	1.05	0.79
T-1	205575	89640	112835	360	1.3907	0.45	0.38	0.31	0.24	0.17
T-2	55937	26017	34163	205	0.3838	0.15	0.13	0.10	0.08	0.05
T-3	67939	26818	28201	315	0.2745	0.22	0.18	0.15	0.12	0.08
T-4	107785	34466	42158	316	0.4996	0.23	0.19	0.16	0.12	0.08
T-5	145800	49879	50124	420	0.7923	0.48	0.41	0.34	0.26	0.19
Ford A-1	862420	272343	274214	848	2.4289	1.19	1.03	0.87	0.71	0.54
Ford B-1	275450	101481	101800	436	0.4101	0.16	0.14	0.11	0.09	0.06
Math B-1	552484	152815	163591	939	0.6388	0.68	0.59	0.50	0.41	0.32
Math D-1	181095	66719	66719	673	0.3457	0.49	0.42	0.35	0.29	0.22
Math E-1	2278011	719372	727232	1294	4.2598	2.07	1.81	1.54	1.27	1.01

TABLE 6

SCHOOL CREEK FIELD - CALCULATED DECLINE CURVE ANALYSIS RESULTS
BASED ON FEDERAL EE-1 PVT (CHANNEL SAND) AND $(\overline{p}_R - p_{wf})/\overline{\mu_o B_o}$ EVALUATION

Well	Pore Vol. V_p RB	Start of Decline OIP STB	OOIP STB	Calculated r_e feet	Prod. Factor $\frac{kh}{\ln \frac{r_e}{r_w'} - \frac{1}{2}}$	s = 0 r_w' = .328 k-md	s = -1 r_w' = .892 k-md	s = -2 r_w' = 2.424 k-md	s = -3 r_w' = 6.588 k-md	s = -4 r_w' = 17.90 k-md
A-1	892968	328988	331621	1138	3.6139	3.07	2.67	2.27	1.87	1.47
C-1	824552	260385	266611	843	0.8197	0.40	0.35	0.29	0.24	0.18
D-2	22683	6208	6208	189	0.0545	0.05	0.04	0.03	0.02	0.01
DD-1	183104	64625	72453	630	1.4752	1.30	1.12	0.93	0.75	0.56
EE-1	346668	101961	115800	620	2.1772	1.28	1.10	0.92	0.73	0.55
F-1	31525	4978	4978	226	0.0733	0.04	0.03	0.03	0.02	0.01
FF-1	73965	30456	38098	301	0.8641	0.55	0.46	0.37	0.29	0.20
G-1	231125	72987	73276	508	0.3945	0.27	0.23	0.19	0.15	0.11
GG-1	707700	223484	227066	1451	1.5704	2.48	2.17	1.85	1.54	1.22
GG-2	384481	121415	121415	626	0.6432	0.32	0.28	0.23	0.19	0.14
H-1	587180	185425	185425	891	0.8319	0.77	0.67	0.56	0.46	0.35
I-1	637459	262483	266322	717	4.7225	2.43	2.09	1.75	1.41	1.08
J-1 (B)	1040805	520402	522163	675	3.6561	1.53	1.32	1.10	0.89	0.67
JJ-1	187219	81164	85451	415	0.5202	0.27	0.23	0.19	0.15	0.11
K-1	1196626	377882	378383	2135	1.1643	2.75	2.42	2.09	1.76	1.42
K-1 (B)	511535	270813	270813	872	2.3648	3.49	3.02	2.55	2.07	1.60
K-4	420053	134060	141520	707	1.5559	1.12	0.96	0.81	0.65	0.49
KK-1	655552	173426	177069	1501	2.3797	4.72	4.12	3.53	2.93	2.34
KK-2	156235	57560	59095	229	0.5687	0.09	0.08	0.06	0.05	0.03
LL-1	57674	19731	21199	279	0.0101	0.01	0.01	.00	.00	.00
LL-2 (B)	128380	52862	56189	580	0.6708	1.17	1.00	0.84	0.67	0.50
O-1	995812	393084	414557	1045	3.5690	2.46	2.13	1.81	1.48	1.16
Q-1	82586	21733	22422	324	0.1798	0.12	0.10	0.08	0.06	0.04
R-1	65831	20789	22424	399	0.1467	0.16	0.14	0.11	0.09	0.06
R-2	52758	16661	17830	280	0.0832	0.05	0.04	0.04	0.03	0.02
R-3	2203310	695782	701225	1936	2.3694	2.77	2.43	2.09	1.75	1.42
R-3 (B)	486739	257686	257686	538	1.3987	0.64	0.55	0.46	0.36	0.27
R-4	338993	107050	119287	677	1.0790	0.77	0.66	0.55	0.45	0.34
S-1	1165131	429259	453792	1075	2.5579	1.62	1.41	1.19	0.98	0.77
S-1 (B)	787611	393805	393805	610	3.8847	1.52	1.30	1.09	0.87	0.65
T-1	169150	73757	96952	326	1.1444	0.37	0.31	0.25	0.19	0.14
T-2	46026	21407	29553	186	0.3158	0.12	0.10	0.08	0.06	0.04
T-3	68966	27223	28606	317	0.2787	0.22	0.19	0.15	0.12	0.08
T-4	90675	28995	36687	289	0.4203	0.19	0.16	0.13	0.10	0.07
T-5	116550	39872	40117	375	0.6334	0.38	0.32	0.26	0.20	0.15
Ford A-1	797412	251814	253685	815	2.2459	1.10	0.95	0.80	0.65	0.50
Ford B-1	220189	81122	81441	390	0.3279	0.13	0.11	0.09	0.07	0.05
Math B-1	418718	115816	126592	817	0.4842	0.51	0.44	0.37	0.30	0.23
Math D-1	153946	56717	56717	620	0.2939	0.41	0.36	0.30	0.24	0.18
Math E-1	2018793	637513	645373	1218	3.7751	1.82	1.59	1.35	1.11	0.88

TABLE 7

SCHOOL CREEK FIELD - CALCULATED DECLINE CURVE ANALYSIS RESULTS
BASED ON MATHESON E-1 PVT (CHANNEL SAND) AND $m(p)_{oil}$ EVALUATION

Well	Pore Vol. V_p RB	Start of Decline OIP STB	OOIP STB	Calculated r_e feet	Prod. Factor $\frac{kh}{\ln \frac{r_e}{r_w'} - \frac{1}{2}}$	s = 0 r_w' = .328 k-md	s = -1 r_w' = .892 k-md	s = -2 r_w' = 2.424 k-md	s = -3 r_w' = 6.588 k-md	s = -4 r_w' = 17.90 k-md
A-1	1104447	525927	528560	1265	7.8542	6.77	5.90	5.02	4.15	3.28
C-1	1144643	467201	473427	994	2.0567	1.03	0.89	0.76	0.62	0.48
D-2	29481	10429	10429	216	0.1297	0.11	0.09	0.07	0.06	0.04
DD-1	318987	129319	137147	832	3.3829	3.10	2.68	2.26	1.83	1.41
EE-1	558453	188666	202505	788	4.7868	2.91	2.51	2.11	1.71	1.31
F-1	35358	7216	7216	240	0.1840	0.10	0.09	0.07	0.05	0.04
FF-1	117453	55930	63572	380	1.9531	1.28	1.09	0.89	0.69	0.50
G-1	272285	111137	111426	552	0.8261	0.57	0.49	0.41	0.32	0.24
GG-1	867284	353993	357575	1607	3.5411	5.66	4.96	4.25	3.54	2.83
GG-2	503362	205454	205454	717	1.5493	0.80	0.68	0.57	0.46	0.35
H-1	834839	340751	340751	1063	2.0874	1.98	1.72	1.46	1.20	0.94
I-1	1189435	562571	566410	980	10.6782	5.72	4.96	4.20	3.43	2.67
J-1 (B)	1198370	599185	600946	725	4.2095	1.78	1.54	1.29	1.04	0.79
JJ-1	315066	159662	163949	539	1.1995	0.64	0.54	0.45	0.36	0.27
K-1	1486687	606811	607312	2380	2.6253	6.29	5.54	4.79	4.04	3.29
K-1 (B)	614938	325555	325555	957	2.8428	4.25	3.68	3.11	2.55	1.98
K-4	603338	246261	253721	848	3.7869	2.79	2.41	2.03	1.65	1.27
KK-1	974655	257845	261488	1830	6.2045	12.61	11.05	9.50	7.95	6.40
KK-2	169018	80485	82020	238	1.4271	0.23	0.19	0.15	0.12	0.08
LL-1	80723	35694	37162	331	0.0254	0.02	0.01	0.01	0.01	0.01
LL-2 (B)	154330	63548	66875	637	0.8064	1.43	1.22	1.02	0.82	0.62
O-1	1243778	634580	656053	1169	7.6629	5.35	4.65	3.96	3.26	2.56
Q-1	111090	37786	38475	377	0.4511	0.30	0.25	0.21	0.16	0.11
R-1	90143	36793	38428	467	0.3680	0.41	0.35	0.29	0.23	0.17
R-2	72243	29487	30656	328	0.2087	0.13	0.11	0.09	0.07	0.05
R-3	2775676	1132929	1138372	2174	5.3427	6.33	5.57	4.81	4.04	3.28
R-3 (B)	585130	309774	309774	590	1.6814	0.78	0.67	0.56	0.45	0.34
R-4	409477	167133	179370	745	2.3849	1.72	1.49	1.25	1.01	0.77
S-1	1514457	721170	745703	1226	5.7677	3.71	3.23	2.75	2.27	1.79
S-1 (B)	930145	465072	465072	663	4.5877	1.81	1.56	1.30	1.05	0.79
T-1	264822	135113	158308	408	2.5262	0.84	0.71	0.58	0.46	0.33
T-2	73983	40263	48409	236	0.6972	0.28	0.24	0.19	0.14	0.10
T-3	81065	41360	42743	344	0.5542	0.45	0.38	0.31	0.24	0.17
T-4	130935	48989	56681	348	0.9091	0.42	0.36	0.29	0.23	0.16
T-5	162061	71660	71905	443	1.5893	0.97	0.82	0.68	0.54	0.39
Ford A-1	968836	395443	397314	898	4.9183	2.43	2.10	1.78	1.45	1.12
Ford B-1	320561	152648	152967	471	0.8227	0.33	0.28	0.23	0.18	0.13
Math B-1	617476	218427	229203	993	1.2054	1.29	1.12	0.95	0.78	0.61
Math D-1	208739	99399	99399	722	0.6806	0.98	0.84	0.71	0.57	0.44
Math E-1	2550551	1041041	1048901	1369	8.5120	4.17	3.64	3.11	2.57	2.04

TABLE 8

SCHOOL CREEK FIELD - CALCULATED DECLINE CURVE ANALYSIS RESULTS
BASED ON MATHESON E-1 PVT (CHANNEL SAND) AND $(\overline{p}_R - p_{wf})/\overline{\mu_o B_o}$ EVALUATION

Well	Pore Vol. V_p RB	Start of Decline OIP STB	OOIP STB	Calculated r_e feet	Prod. Factor $\frac{kh}{\ln \frac{r_e}{r_w'} - \frac{1}{2}}$	s = 0 r_w' = .328 k-md	s = -1 r_w' = .892 k-md	s = -2 r_w' = 2.424 k-md	s = -3 r_w' = 6.588 k-md	s = -4 r_w' = 17.90 k-md
A-1	898346	427784	430417	1141	6.3885	5.43	4.72	4.01	3.30	2.59
C-1	755925	308541	314767	807	1.3583	0.66	0.57	0.48	0.39	0.30
D-2	20959	7414	7414	182	0.0922	0.08	0.06	0.05	0.04	0.02
DD-1	228179	92505	100333	703	2.4199	2.17	1.87	1.56	1.26	0.96
EE-1	427729	144503	158342	689	3.6663	2.18	1.88	1.57	1.27	0.96
F-1	23350	4765	4765	194	0.1215	0.07	0.05	0.04	0.03	0.02
FF-1	87951	41882	49524	329	1.4626	0.94	0.79	0.65	0.50	0.35
G-1	241168	98436	98725	519	0.7317	0.50	0.43	0.36	0.28	0.21
GG-1	669523	273275	276857	1412	2.7337	4.30	3.75	3.21	2.66	2.11
GG-2	351874	143622	143622	599	1.0831	0.54	0.46	0.39	0.31	0.23
H-1	551330	225033	225033	864	1.3786	1.27	1.10	0.93	0.75	0.58
I-1	868886	410959	414798	837	7.8005	4.09	3.54	2.98	2.42	1.86
J-1 (B)	1040805	520402	522163	675	3.6561	1.53	1.32	1.10	0.89	0.67
JJ-1	226419	114739	119026	457	0.8621	0.45	0.38	0.31	0.25	0.18
K-1	1147688	468444	468945	2091	2.0267	4.78	4.20	3.62	3.05	2.47
K-1 (B)	511535	270813	270813	872	2.3648	3.49	3.02	2.55	2.07	1.60
K-4	394845	161161	168621	685	2.4783	1.77	1.52	1.28	1.03	0.78
KK-1	679465	179753	183396	1528	4.3254	8.59	7.51	6.43	5.35	4.27
KK-2	111620	53152	54687	193	0.9425	0.15	0.12	0.10	0.07	0.05
LL-1	53310	23572	25040	268	0.0168	0.01	0.01	0.01	0.01	.00
LL-2 (B)	128380	52862	56189	580	0.6708	1.17	1.00	0.84	0.67	0.50
O-1	1044348	532831	554304	1070	6.4343	4.44	3.85	3.27	2.69	2.10
Q-1	73364	24954	25643	306	0.2979	0.19	0.16	0.13	0.10	0.07
R-1	59530	24298	25933	379	0.2431	0.27	0.22	0.18	0.14	0.10
R-2	47709	19473	20642	266	0.1379	0.09	0.07	0.06	0.04	0.03
R-3	2142759	874595	880038	1909	4.1245	4.81	4.22	3.64	3.05	2.46
R-3 (B)	486739	257686	257686	538	1.3987	0.64	0.55	0.46	0.36	0.27
R-4	324438	132424	144661	662	1.8896	1.34	1.15	0.97	0.78	0.59
S-1	1169126	556727	581260	1077	4.4526	2.82	2.45	2.08	1.71	1.33
S-1 (B)	787611	393805	393805	610	3.8847	1.52	1.30	1.09	0.87	0.65
T-1	205561	104878	128073	359	1.9609	0.64	0.54	0.44	0.34	0.25
T-2	57427	31253	39399	208	0.5412	0.21	0.18	0.14	0.11	0.07
T-3	67547	34463	35846	314	0.4618	0.37	0.31	0.25	0.19	0.14
T-4	106495	39845	47537	313	0.7395	0.34	0.28	0.23	0.18	0.12
T-5	107026	47324	47569	360	1.0496	0.62	0.52	0.43	0.33	0.24
Ford A-1	779935	318341	320212	806	3.9593	1.93	1.66	1.40	1.14	0.87
Ford B-1	211699	100809	101128	382	0.5433	0.21	0.18	0.15	0.11	0.08
Math B-1	404097	142946	153722	803	0.7889	0.82	0.71	0.60	0.48	0.37
Math D-1	150804	71811	71811	613	0.4917	0.69	0.59	0.50	0.40	0.30
Math E-1	1989906	812207	820067	1209	6.6410	3.20	2.79	2.37	1.96	1.54

SPE 14237

TABLE 9

EXAMPLE OF EFFECT OF BACKPRESSURE CHANGE ON DECLINE AND RECOVERY
FEDERAL A-1

$\bar{p}_R$ = 3500 psi; p_b = 2705 psi

Match Point, b = 0.30:

q(t) = 1000 BOPM; q_{Dd} = 0.220

t = 1 mo; t_{Dd} = 0.212

$$q_i = \frac{1000 \text{ BOPM}}{0.220} = 4545.5 \text{ BOPM}; \quad D_i = \frac{0.212}{1 \text{ mo}} = 0.212 \text{ mo}^{-1}$$

$$q(t) = \frac{q_i}{[1 + bD_i t]^{1/b}} = \frac{4545.5 \text{ BOPM}}{[1 + 0.0636t]^{3.333}}$$

First backpressure change 1400 psia to 1069 psia @ t = 11 months

q_1 @ t = 1 mo = 3701 BOPM (See Figure 9)

$$\Delta q_1 = q_1 \frac{\left[\dfrac{p_{wf_1}^{\;2} - p_{wf_2}^{\;2}}{2p_b}\right]}{\left[(\bar{p}_R - p_b) + \dfrac{(p_b^{\;2} - p_{wf_1}^{\;2})}{2p_b}\right]} = 3701 \frac{\left[\dfrac{1400^2 - 1069^2}{2(2705)}\right]}{\left[(3500 - 2705) + \dfrac{(2705^2 - 1400^2)}{2(2705)}\right]} = 313 \text{ BOPM}$$

Second Backpressure change 1069 psia to 100 psia @ t = 16 months

$$\Delta q_2 = q_1 \frac{\left[\dfrac{p_{wf_2}^{\;2} - p_{wf_3}^{\;2}}{2p_b}\right]}{\left[(\bar{p}_R - p_b) + \dfrac{(p_b^{\;2} - p_{wf_1}^{\;2})}{2p_b}\right]} = 3701 \frac{\left[\dfrac{1069^2 - 100^2}{2(2705)}\right]}{\left[(3500 - 2705) + \dfrac{(2705^2 - 1400^2)}{2(2705)}\right]} = 434 \text{ BOPM}$$

TABLE 9-A

EXAMPLE OF EFFECT OF BACKPRESSURE CHANGE ON DECLINE AND RECOVERY
FEDERAL A-1

	[1] t	[2] q_1	[3] Δq_1	[4] Δq_2	[5] Column [3] @ t = 12 mo	[6] Column [4] @ t = 17 mo	[7] q Total [2]+[5]+[6]
			$\left\{\frac{313}{3701} \times [2]\right\}$	$\left\{\frac{434}{3701} \times [2]\right\}$			
	mo	BOPM	BOPM	BOPM	BOPM	BOPM	BOPM
p_{wf_1}	1	3701	313	434			3701
	2	3050	258	358			3050
	3	2540	215	298			2540
	4	2135	181	250			2135
	5	1811	153	212			1811
	6	1548	131	181			1548
	7	1332	113	156			1332
	8	1154	98	135			1154
	9	1006	85	118			1006
	10	881	75	103			881
p_{wf_2}	11	776	66	91			776
	12	687	58	81	313		1000
	13	610	52	72	258		868
	14	544	46	64	215		759
	15	487	41	57	181		668
p_{wf_3}	16	438	37	51	153		591
	17	395	33	46	131	434	960
	18	357	30	42	113	358	828
	19	324	27	38	98	298	720
	20	295	25	35	85	250	630
	.	.	.	.	.	.	.
	.	.	.	.	.	.	.
	.	.	.	.	.	.	.
	58	26	2	3	4	7	37
	59	25	2	3	4	7	36
	60	24	2	3	4	6	34
	61	23	2	3	3	6	32
	62	22	2	3	3	6	31
Cum (BO):		27,714	2,344	3,250	2,320	3,191	33,225

TABLE 10

SUMMARY OF SCHOOL CREEK FIELD OOIP AND ULTIMATE RECOVERY

	Can Include Flowing Pressure Changes						Initial p_{wf_1}	
	$m(p)_{oil}$			$(\bar{p}_R - p_{wf})/(\mu_o B_o)$				
Well	OOIP STB	Ultimate Reserves Forecast STB	Recovery Factor Percent	OOIP STB	Ultimate Reserves Forecast STB	Recovery Factor Percent	Ultimate Reserves Forecast STB	
A-1	528560	33719	6.4	430417	44270	10.3	28606	Channel Sand Matheson E-1 PVT
C-1	473427	26692	5.6	314767	26692	8.5	26692	
D-2	10429	1032	9.9	7414	1032	13.9	1032	
(P&A) F-1	7216	848	11.8	4765	848	17.8	848	
G-1	111426	6343	5.7	98725	9309	9.4	4256	
JJ-1	163949	11122	6.8	119026	12120	10.2	10885	
K-4	253721	21282	8.4	168621	21282	12.6	21282	
Q-1	38475	3357	8.7	25643	3357	13.1	3357	
R-1	38428	3988	10.4	25933	3988	15.4	3988	
R-2	30656	2063	6.7	20642	2063	10.0	2063	
Ford A-1	397314	27538	6.9	320212	35289	11.0	24096	
Ford B-1	152967	8909	5.8	101128	8909	8.8	8909	
Math B-1	229203	22107	9.6	153722	22107	14.4	22107	
Math D-1	99399	5662	5.7	71811	5662	7.9	5662	
Math E-1	1048901	64832	6.2	820067	78333	9.6	60117	
Sub Totals	3584071	239494	6.7	2682893	275261	10.3	223900	
DD-1	92310	14182	15.4	72453	15040	20.8	13967	Channel Sand Federal EE-1 PVT
EE-1	142234	23130	16.3	115800	25841	22.3	22091	
FF-1	45148	9430	20.9	38098	9911	26.0	9295	
GG-1	253505	28527	11.3	227066	34233	15.1	26719	
GG-2	145704	13280	9.1	121415	14300	11.8	13131	
H-1	231961	22243	9.6	185425	22243	12.0	22243	
I-1	342150	57238	16.7	266322	64346	24.2	54423	
KK-1	187379	19050	10.2	177069	31051	17.5	15018	
KK-2	73541	13769	18.7	59095	13769	23.3	13769	
LL-1	26150	3472	13.3	21199	3472	16.4	3472	
O-1	435740	46069	10.6	414557	60449	14.6	39046	
R-4	130371	21311	16.3	119287	22919	19.2	20205	
T-1	112835	28751	25.5	96952	30268	31.2	28229	
T-2	34163	7925	23.2	29553	8341	28.2	7782	
T-3	28201	7352	26.1	28606	7352	25.7	7352	
T-4	42158	9431	22.4	36687	10010	27.3	9198	
T-5	50124	6165	12.3	40117	6165	15.4	6165	
Sub Totals	2373674	331325	14.0	2049701	379710	18.5	312105	
J-1 (B)	600946	53769	8.9	522163	70643	13.5	45938	Bar and Channel PVT
K-1 (B+C)	932867	59999	6.4	739758	73780	10.0	55315	
LL-2 (B)	66875	12373	18.5	56189	13421	23.9	12025	
R-3 (B+C)	1093312	109671	10.0	1137724	134702	11.8	96732	
S-1 (B+C)	969646	81207	8.4	975065	102313	10.5	73469	
Sub Totals	3663646	317019	8.7	3430899	394859	11.5	283479	
Grand Totals	9621391	887838	9.2	8163493	1049830	12.9	819484	

Total Percent Recovery Factor = Total Reserves ÷ Total OOIP

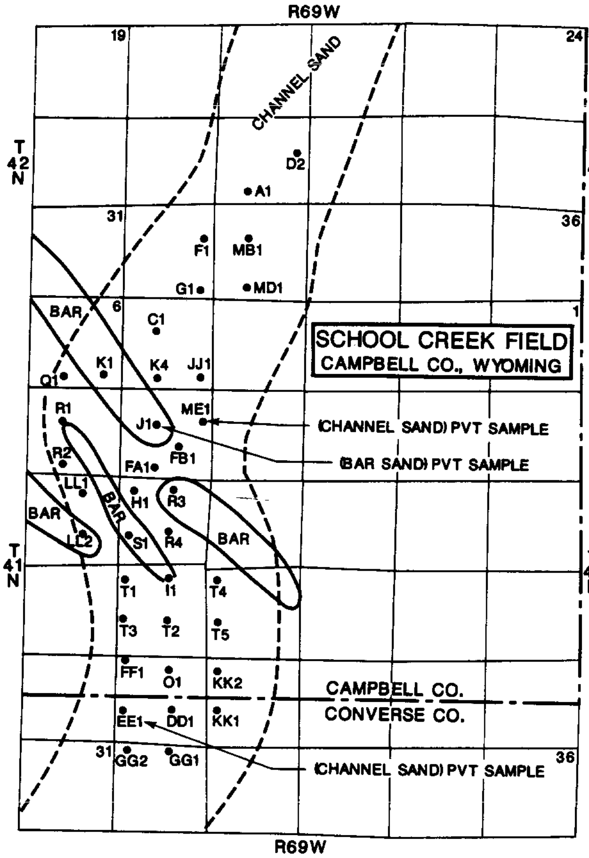

Fig. 1—School Creek field well location map.

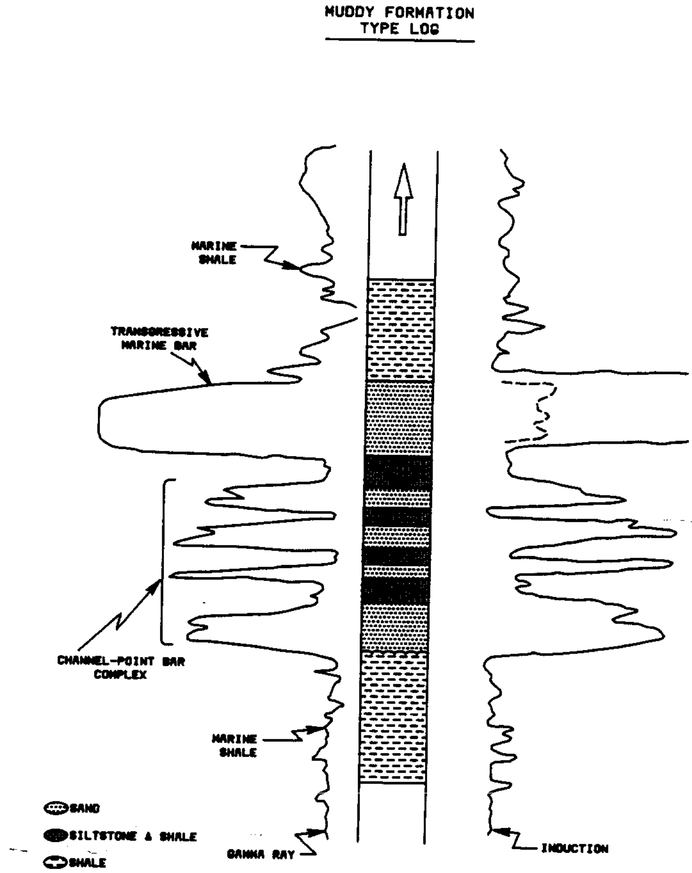

Fig. 2—Type log for a Muddy formation completion.

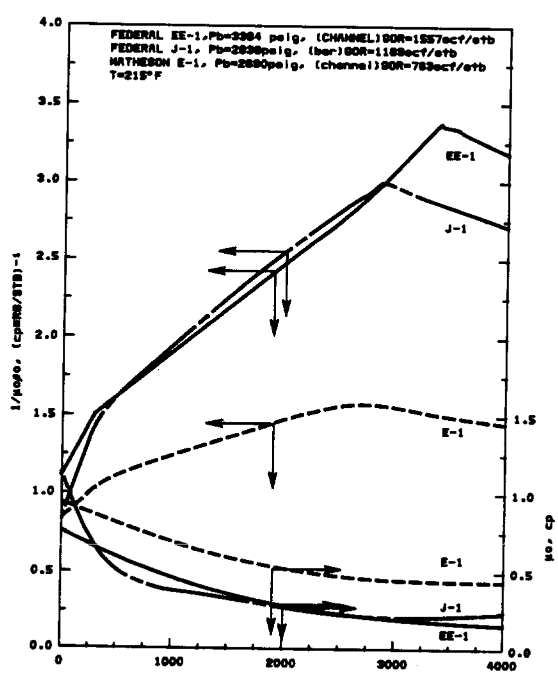

Fig. 3—PVT samples from the School Creek field.

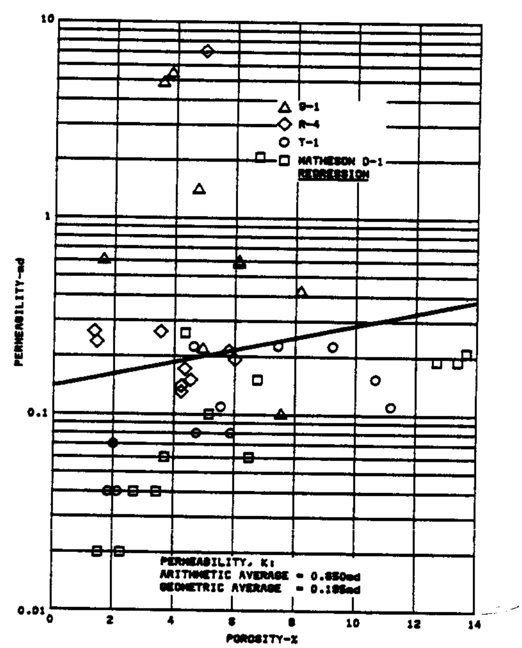

Fig. 4—Porosity-permeability results from core analysis.

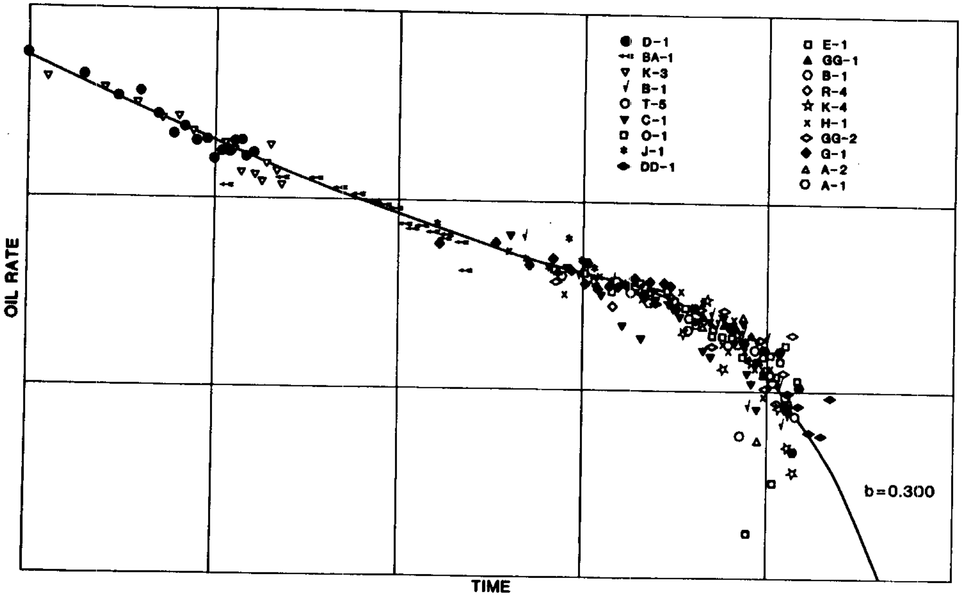

Fig. 5—Initial School Creek field log-log type curve.

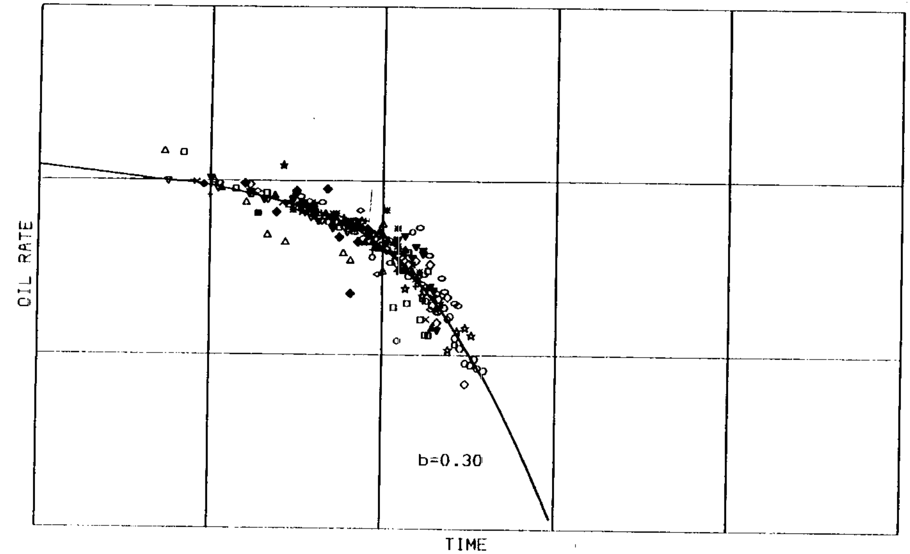

Fig. 6—Final School Creek field log-log type curve.

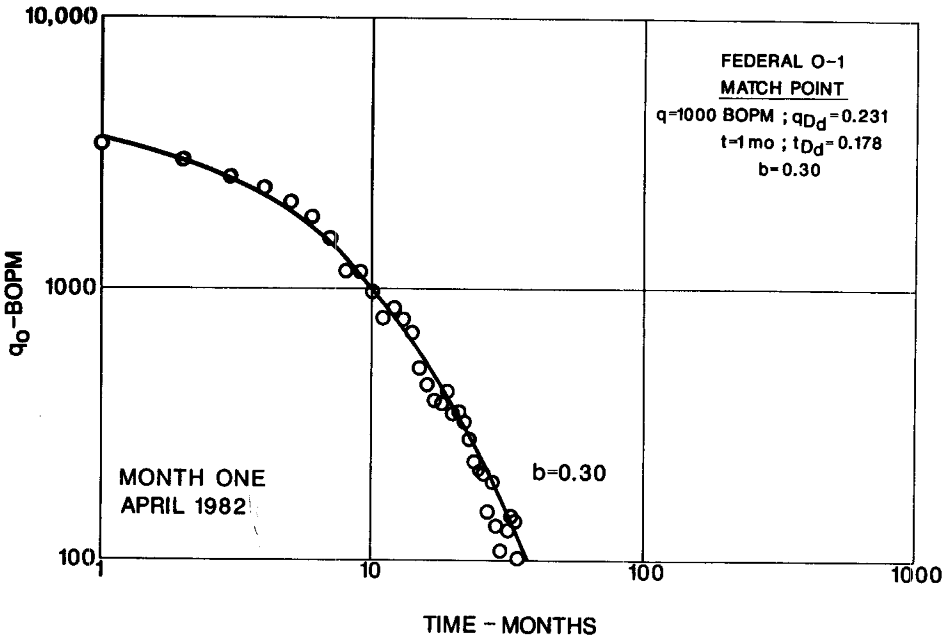

Fig. 7—Decline exponent b = 0.30 established from rate-time data.

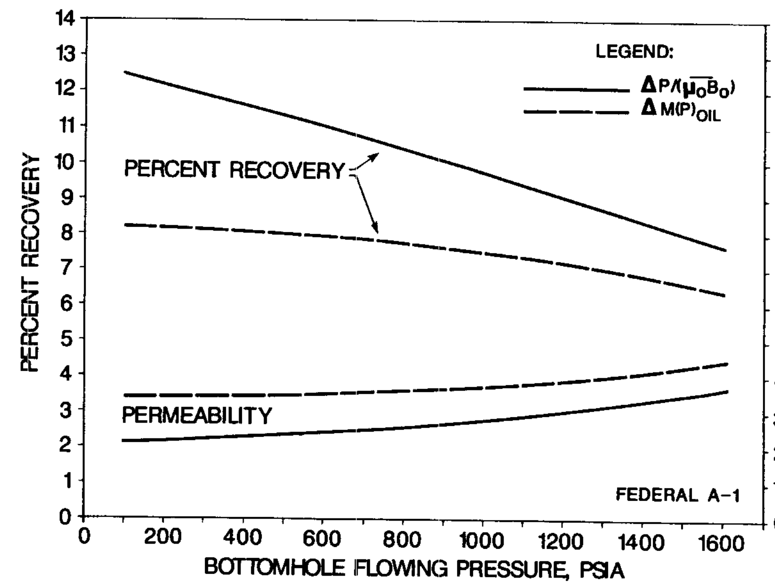

Fig. 8—Sensitivity of calculated percent recovery and permeability to bottomhole flowing pressure.

SPE 14237

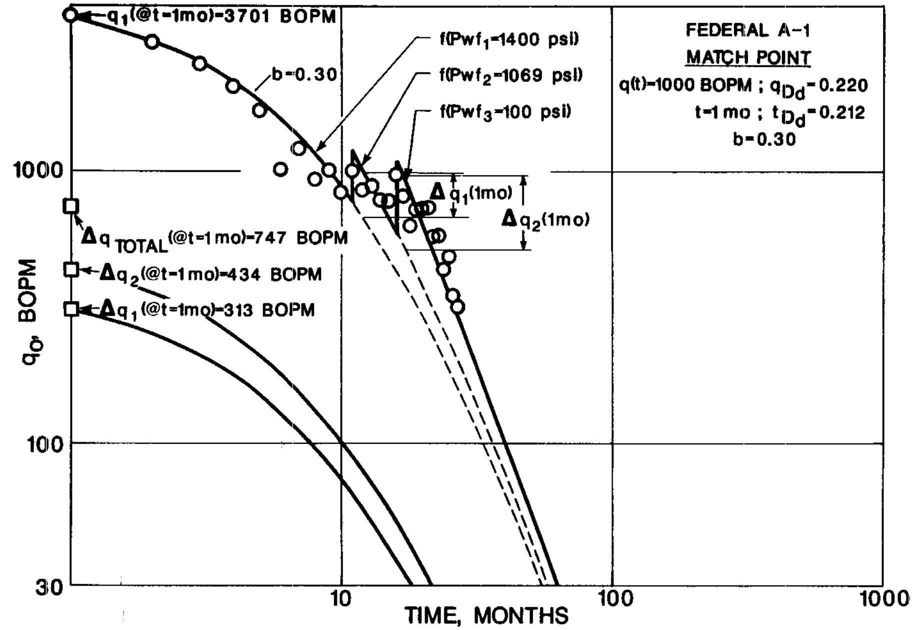

Fig. 9—Example of effect of backpressure changes on recovery.

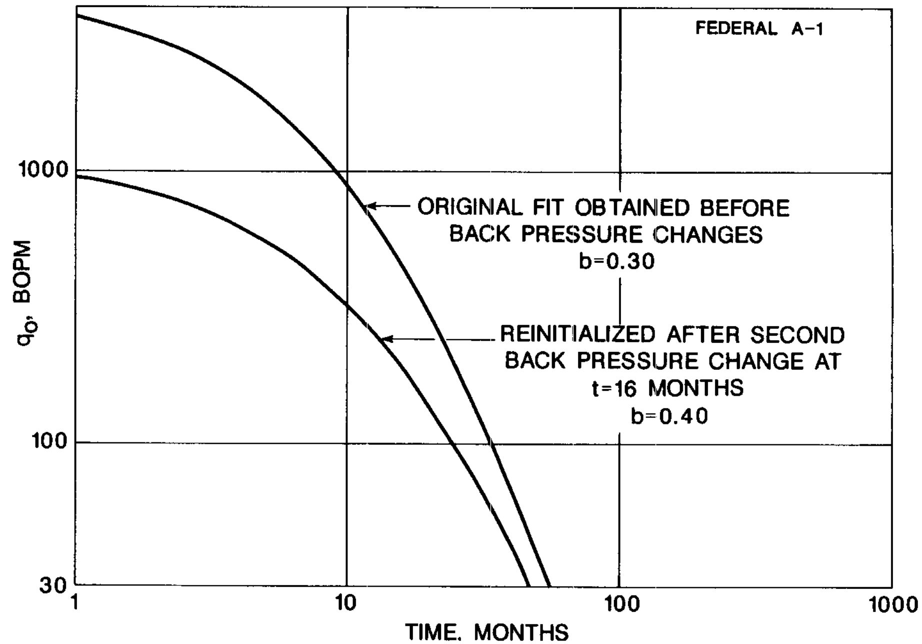

Fig. 10—Effect of backpressure changes on decline exponent, b.

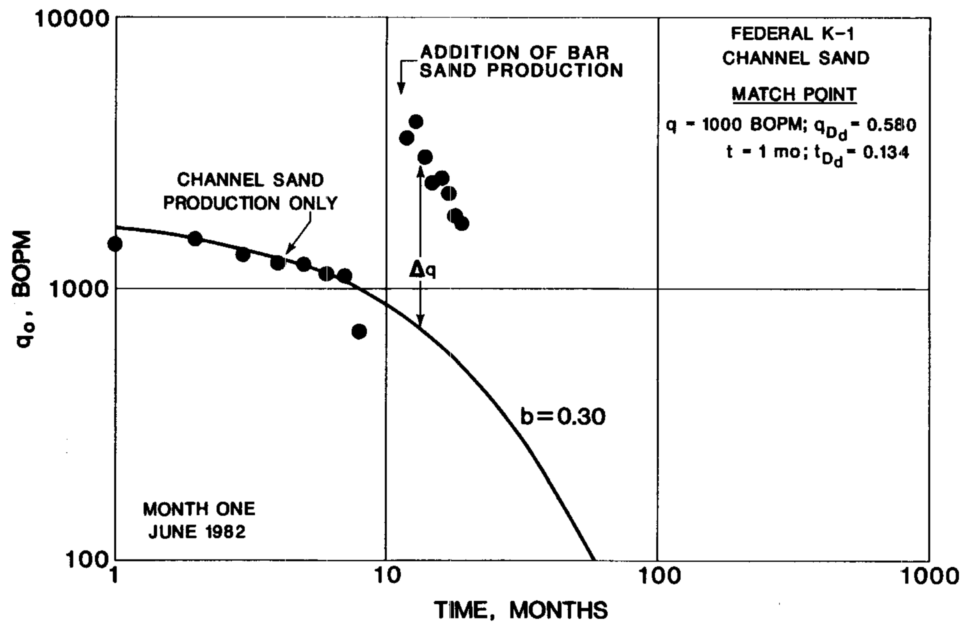

Fig. 11—Rate-time data for a well commingled with another reservoir.

SPE 14237

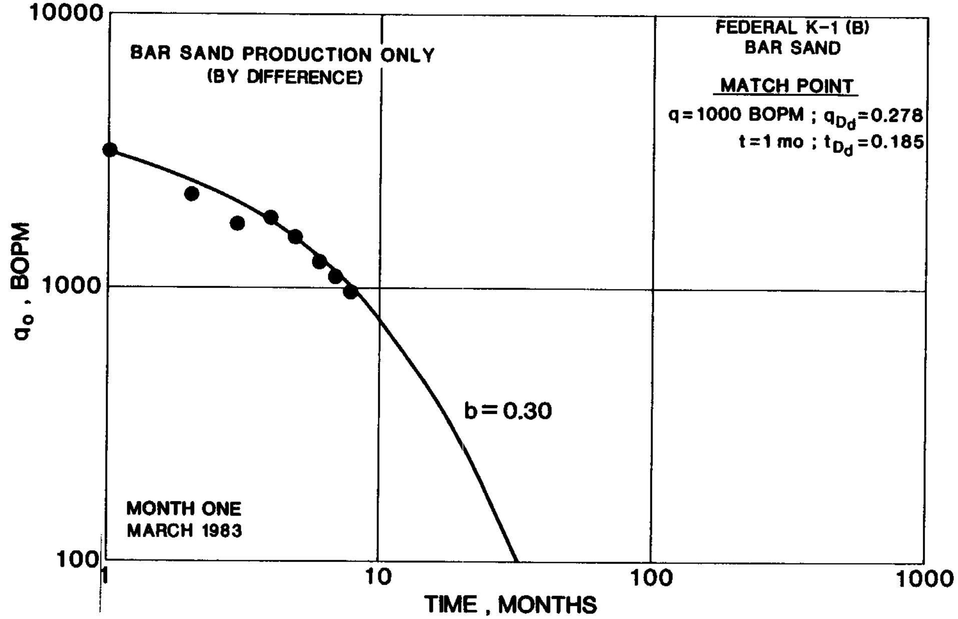

Fig. 12—Decline data for a commingled well established by difference in production.

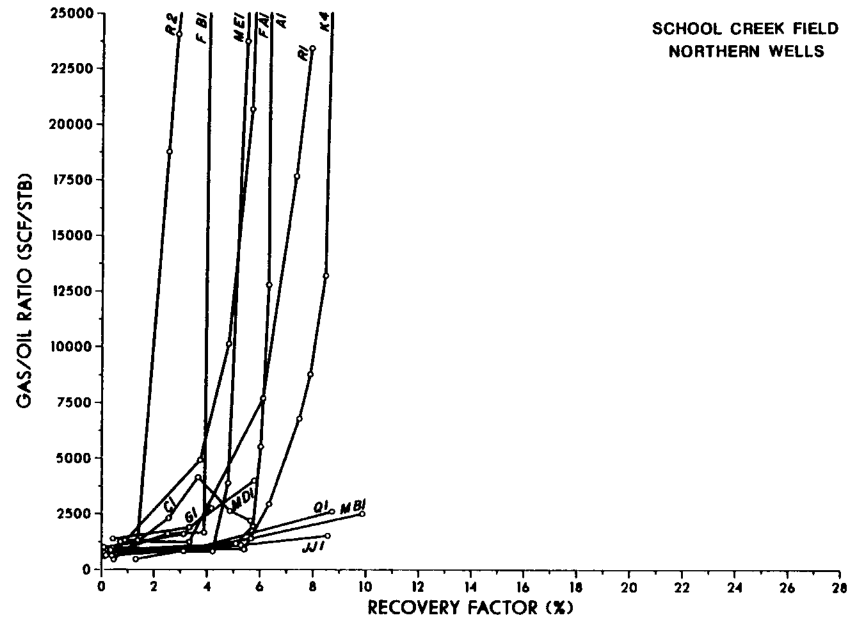

Fig. 13—Individual well GOR performance, based on m(p) calculated OOIP.

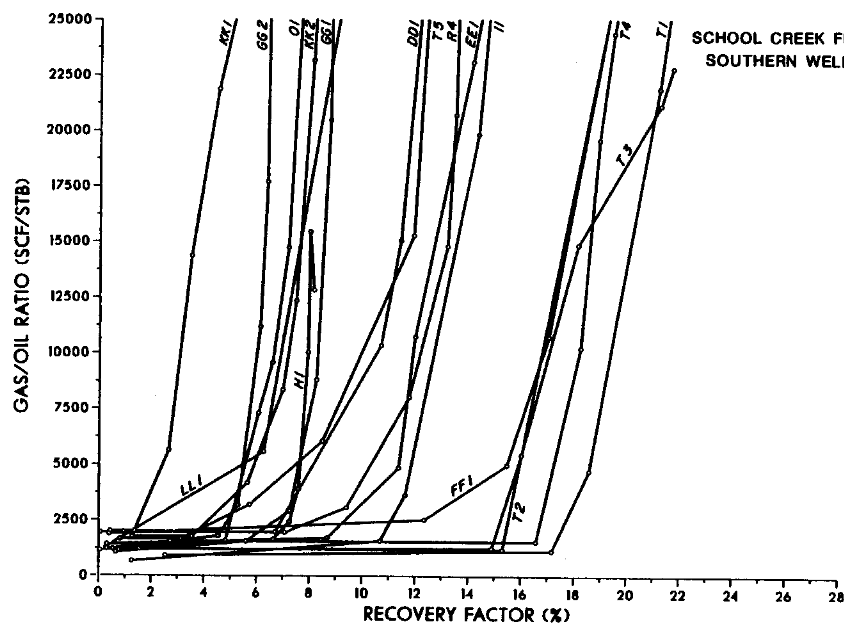

Fig. 14—Individual well GOR performance, based on m(p) calculated OOIP.

SPE 14237

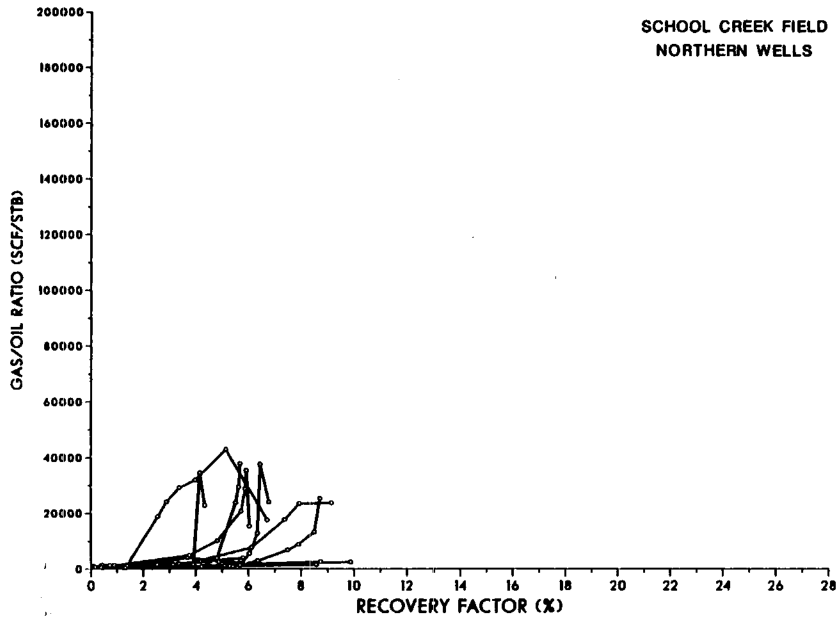

Fig. 15—Individual well peak GOR performance, based on m(p) calculated OOIP.

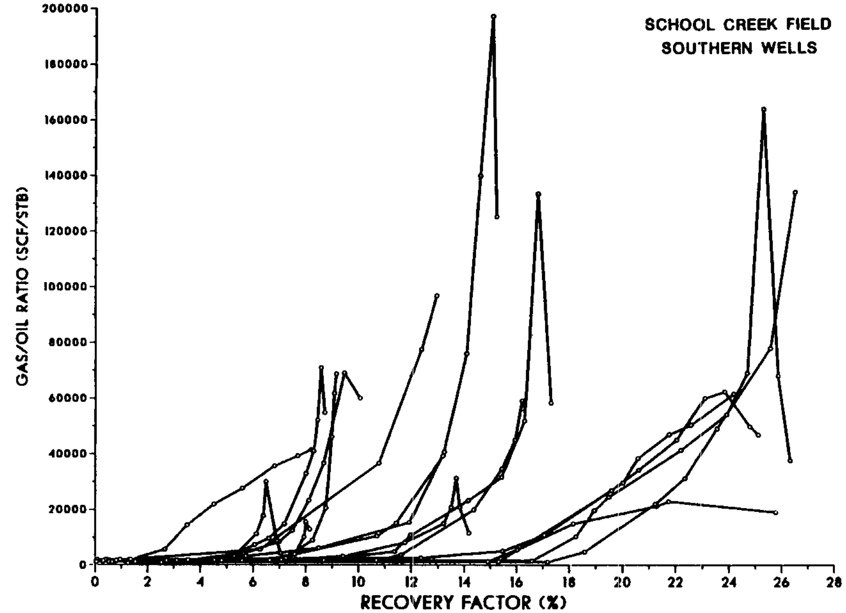

Fig. 16—Individual well peak GOR performance, based on m(p) calculated OOIP.

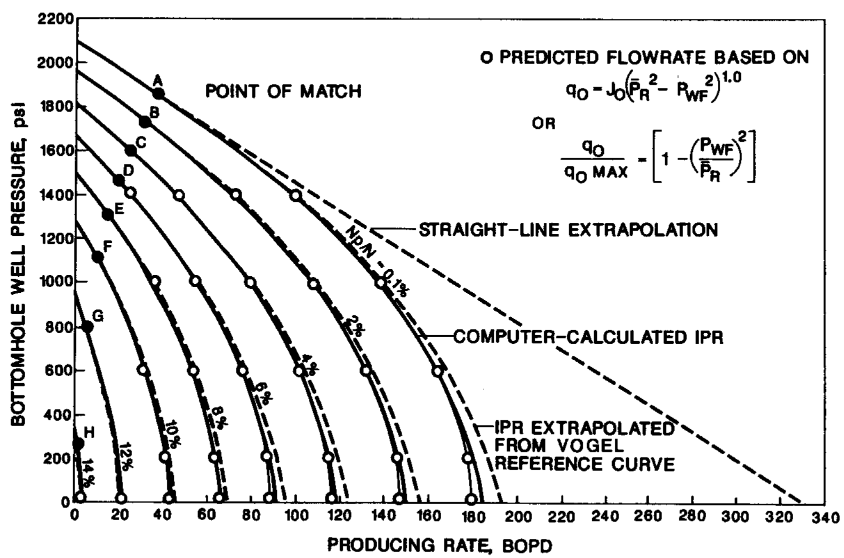

Fig. 17—Comparison of inflow performance equations.

SPE 14237